

Conservation of Subterranean Historic and Prehistoric Monuments

The Importance of the Environment and Microclimate

Jacques Brunet, Jean Vouvé, and Philippe Malaurent

THE PREHISTORIC DECORATED CAVES found in France, formed by the weathering of calcareous rock, are generally the result of morphological, structural accidents. Before they were found, these caves were either totally isolated from the outside world or, in some cases, discernible only through tiny fissures or openings. Environmental conditions maintained over long periods of isolation—several thousand years in the case of some upper Paleolithic caves—have determined what types of rock art remain visible today.

Following the discovery of these caves and the greater appreciation of prehistoric art they engendered, access to them was provided by cutting openings through blocks of fallen or crumbled rock that had built up over the millennia. This new access has disturbed the caves' natural, subterranean environment, which had remained stable prior to intervention, and has also disturbed the rock art they contain.

The purpose of the following discussion is to explore the requirements for conserving natural, subterranean sites and to apply the results of these investigations to specific examples. It is hoped that knowledge gained by studying carbonate rock might also shed light on the problems of tombs, tumuli, and other subterranean natural, prehistoric, or historic monuments.

Factors Affecting the Stability of Paintings and Engravings in the Subterranean Environment

The atmosphere

Like aerial space, subterranean space has its own defined character. Its internal climate can be influenced either directly or indirectly by the external climate. Variations in temperature, atmospheric pressure, environment, and different density levels of the interior space generate air movement and exchange with the exterior. The exchange in both directions takes place either continuously within the atmospheric domain or more indirectly through the porous and permeable geological matter, such as the cave rock itself, fallen rocks, earth, or karstic infilling. The atmosphere of a cave or buried monument is established by its geomorphology,

position, and depth in the ground (Schoeller 1972; Vouvé et al. 1983).

Depending on the surrounding natural context, the cave may be subject to air exchanges, both thermal and hydrogeological, that emanate from the surface but take some time to diffuse. When a cave is superficial (extending less than 25 m into the ground), temperature differences and variation in air flows may depend on the following:

- general layout of the cave entrance (morphology, exposure, altitude);
- geometry and nature of any geological aquifer or reservoir in relation to the subterranean space; and
- geometry of the cave space itself (horizontal, descending, or ascending).

One recent and very important consideration is the effect of tourism on ancient decorated caves. Studies have shown that each visitor introduces 40 g of water vapor, 20 l of CO₂, and 250 J hour⁻¹ into the subterranean environment. These moisture, gas, and thermal intrusions destabilize the interior environment of the cave. Visitors also introduce the risk of biological contamination by microorganisms, such as algae, bacteria, and fungi, which grow rapidly in a subterranean environment. Mineral salts and organic matter are other problems created by the respiration and transpiration of visitors, who also produce a dust layer on the wall surfaces as they walk across the ground.

To this list of tourist-induced hazards may be added the increased exterior-interior air exchanges that take place as visitors come and go, and the effects of heating from artificial lights, which are constantly in use during tourism periods.

Cave rock

Bare rock provides the support base for decorated cave walls, the surfaces of which have been formed and shaped by natural erosion. In general, the limestone or sandstone rock has not been modified by tools or mortar. A consideration of the physical characteristics of the rock—its cracks, water content resulting from direct or delayed infiltration, and chemical qualities (such as salt and mineral content)—should influence the decisions made in conserving a subterranean environment.

Location of paintings and engravings

Painted and engraved rock art is situated at the interface between rock and air, and it is affected by the physicochemical mechanisms that develop there. Thermal exchanges with the interface (rock-water, rock-air, air-water) and dynamic exchanges between the exterior and subterranean environments cause water and air migration into underground caves that, in turn, produce condensation or evaporation. In limestone caverns, all these mechanisms have both favorable and adverse effects on calcite formations.

The mechanical stability of a cave's inner walls and decorations (as well as the surfaces of most archaeological objects) is dependent essentially on humidity level. A sudden and significant dehydration of the surface will impair the cohesion of pigments and mortar. In the same way, significant condensation will form a permanent water film, which fosters the development of harmful bacteria and algae. Condensation trickling down a wall's surface eventually leads to deterioration and loss of paintings and decoration.

Given these conditions, safeguarding the subterranean environment with its art and artifacts requires nothing less than actual atmospheric control, with tourist visits limited to five persons per day.

Evaporation-Condensation and Conservation of Subterranean Environments

Only a few environmental parameters can be measured with certainty:

- temperature of the external air
- relative humidity of the external air
- atmospheric pressure of the external air
- temperature of the air inside the space
- relative humidity of the air inside the space
- atmospheric pressure of the air inside the space
- temperature of the inner wall surfaces

The air mass of a cavity of temperature T_a , in contact with the inner wall of temperature T_p , is subject to the physical laws of condensation and evaporation. Thus, when the air's water-vapor pressure is greater than its saturated water-vapor pressure (at the same temperature as the wall surface), a film of water will appear as a result of condensation. Characteristics of this wet film vary, depending on the air mixture at the wall surface, the makeup of this surface, and its porosity. Unfortunately, these factors are almost impossible to calculate. Likewise, if the air's water-vapor pressure is lower than the saturated vapor pressure (at the same temperature as the wall surface), water will evaporate from the wall. How will this condensation and evaporation affect the support surface?

In climates where rainfall lasts from a few weeks to several months of the year, the water exchange (vapor-liquid) within the heart of the rock and at the interface with the atmosphere leads invariably to deterioration. The problem of evaporation-condensation and the response this causes on the interface is the main issue here (Stefanaggi, Vouvé, and Dangas 1986; Malaurent, Vouvé, and Brunet 1993).

In each of the following examples, droughts, intense rain, or other exceptional weather patterns—as well as structural work—are at the root of the microclimatic processes. These conditions cause an imbalance between the water-vapor pressure in the air and at the interface, resulting in either a physical or a physicochemical reaction on decorated and undecorated surfaces. In the following case studies of moisture imbalances, A and A' refer to decorated caves and shelters; B refers to archaeological sites (Fig. 1).

Figure 1

Caves (A), decorated shelters (A'), and covered archeological sites (B) all have their own particular microclimate: 1 = calcareous fissures; 2 = impermeable calcareous clay; 3 = sand infilling; 4 = paintings; 5 = sandy clay alluvial deposits; 6 = archeological objects; 7 = alveolar concrete vaults; 8 = water table.

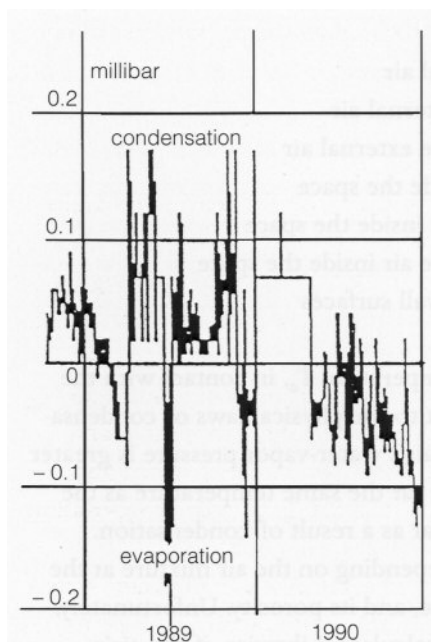
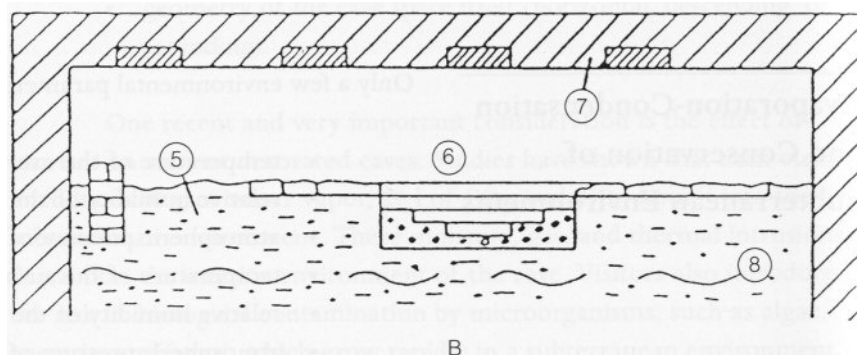
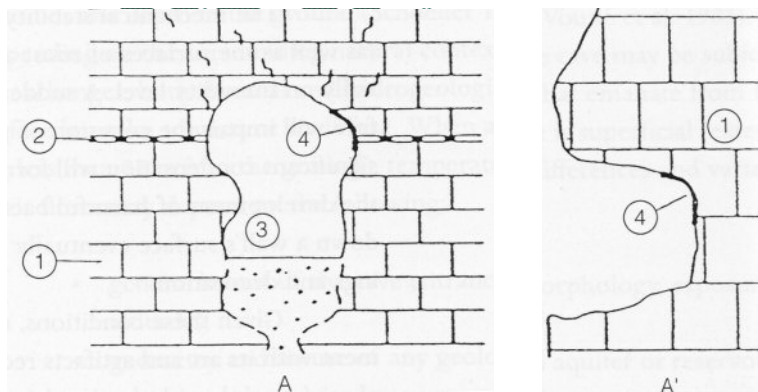


Figure 2
Diagram showing evaporation-condensation phenomena in the case of a cave; analysis was carried out between 1989 and 1990.

The first three examples present cases in which the water-vapor pressure at the carbonate (or similar type) wall surfaces is greater than the more balanced pressure of the surrounding air.

Cases A and A': Cave or rock shelter

In a cave or rock shelter excavated in limestone, water that is present at the interface (in the form of a film or droplets) and that is in chemical equilibrium with the calcitic facies will evaporate (Fig. 2). This calcite formation takes place under a variety of polymorphic conditions, the main micromorphologic patterns of which are shown in Table 1 (evaporatory conditions). An example of needles grafted onto preformed buds is shown in Figure 3. Methods used to obtain visual images and automatic

Figure 3
Growth of calcite crystals on a prehistoric painting.

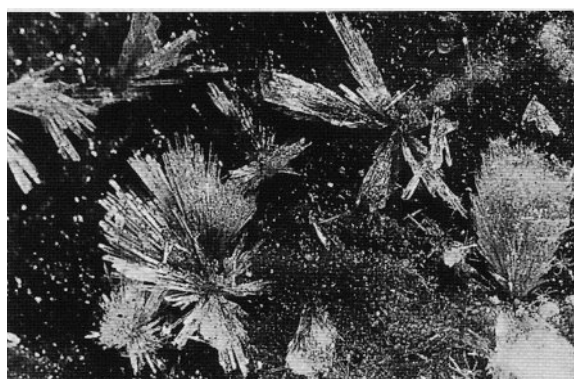


Table 1 Identification of growth and dissolution of calcite crystals influenced by evaporation-condensation phenomena, as seen in decorated caves or shelters

Growth phase (polymorphism) (evaporatory conditions)	Dissolution phase (condensation conditions)
<ul style="list-style-type: none"> • Single (pinpointed), clusters, larger areas precipitates: amorphous • Simple, complex growth (chaotic, massive) • Needles grafted onto flat or "conchoidal" supports • Pointed budding disorganized, organized, thin layers, flakes 	<ul style="list-style-type: none"> • Forming of craters or pits (craterization) • Ablations (tips of needles and microdroplets) • Flaking • Swellings and loss of cohesion

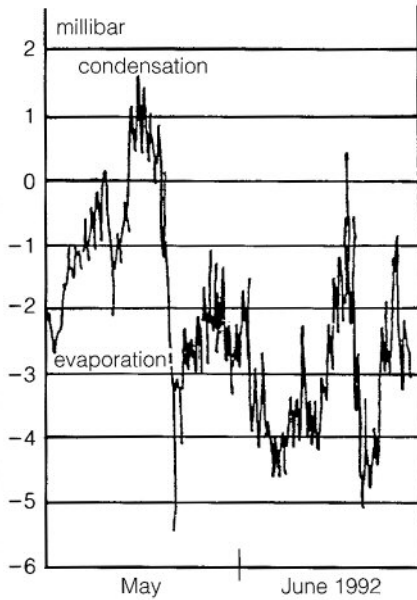


Figure 4 Diagram showing the evaporation-condensation phenomena in the case of an artificially covered archeological site. Analysis was carried out in May and June 1992.

processing of these data make it possible to follow the phenomena of crystal growth stage by stage.

Case B: Burial vault

In a monument such as a concrete burial vault with the same evaporatory atmosphere as a cave (Fig. 4), the saturated or capillary water content of the walls' stone or mortar (or other porous or permeable archaeological elements) migrates toward the interface where it eventually evaporates (see Fig. 5, walls M1 and M2). This phenomenon sometimes includes chemical precipitates and often entails loosening of mortar, joints, and other coatings. It is also often accompanied by flaking, powdering, and bleaching of the colored areas, which may be made up of crushed and compressed brick. In Figure 5, the effects (bleaching) of water evaporation are shown coming from the walls (M1 or M2) through the floor.

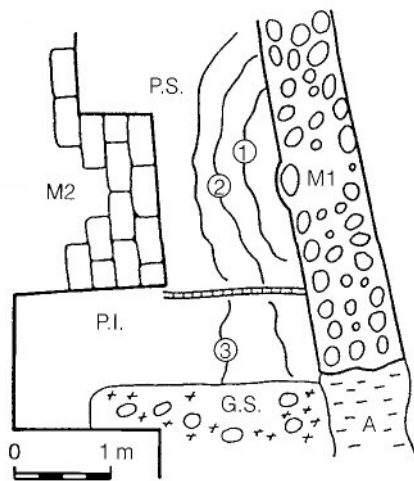


Figure 5 Ground plan of the excavation: P.S. = higher floor; P.I. = lower floor; M1 and M2 = eroded historic walls; A = clays; G.S. = shingle. Map of the observed increase of the bleaching area (salts) at different periods of time: line 1 = 31 March 1993; line 2 = 1 June 1992; line 3 = 22 September 1992. Lines 1, 2, and 3 are the limits of the bleaching area.

The next three examples represent cases in which the water-vapor pressure of the wall surfaces is lower than that of the surrounding air. In A and A' (cave or rock shelter), the water vapor of the subterranean atmosphere condenses on the surfaces and/or the calcite formed on the vaults of an enclosed space. Continual condensation over the years (Fig. 2) has created a constant supply of water, thousands of microscopic droplets that enlarge and merge. Methods used to obtain visual images and automatic processing of these data make it possible to identify these droplets, especially when they appear on a painted support (Fig. 6). Depending on the calcitic micromorphology, the interaction of these droplets with each other may lead to water flow. This, in some cases, leads to leaching loss and dispersion of organic (wood charcoal) or mineral pigments in wall paintings. Preventive measures are essential if the wall paintings and rock art are to be conserved. It is also important to note that in situations where the wall is homogeneously wet, without flowing, the effect of the film of water increases the visibility of the painted layers.

Case B is an example of an urban archaeological site with wall constructions and overlapping flooring built on fine silt, sandy clay, and coarse gravel alluvial deposits that are extremely close to the middle level

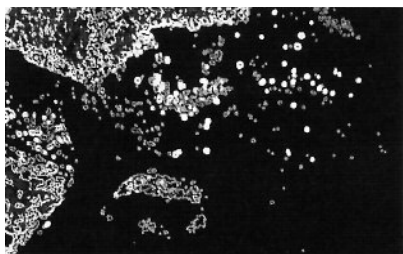


Figure 6
Parietal condensation droplets on a painted support, Lascaux.

A Controlled Subterranean Environment: The Cave of Lascaux

of the alluvial water table. This site has been reinforced by the construction of a ring of walls and also has been covered over by a concrete slab.

The surrounding archaeological excavation remains active for eight hours per day. Continuous recordings of the ground temperature and subterranean air and wall temperatures, as well as the air hygrometry, make it possible to calculate the imbalance between the water-vapor pressures in real terms. An air-extracting pump may be employed to dry the air, if necessary. In cases where condensation is developing (Fig. 4), it is possible to follow the moisture content of the wall surface (in this case, of a vault) by mapping the visual observations of the state of the site. Observations over time show increases and growth in the droplets that form on the recesses of the horizontal vault (Fig. 7a, b). These droplets lower the energy barrier necessary for the formation of a liquid-vapor interface. Small, separate droplets increase in size at the expense of the vapor, then merge; when they have reached their maximum size, they fall off and soak the ground, as well as structures and archaeological objects. The cycle of evaporation from the ground and condensation on the vault leads to destabilization of poorly adhered materials.

Since its discovery in 1940, the cave of Lascaux has been subject to a number of adverse circumstances, making it a very complex model (Fig. 8a, b). Situated at a depth of 0–25 m below ground (Fig. 9), this cave highlights the problems of conserving original works of art and necessitates a definition of the ideal subterranean climate (Figs. 10–12). The restoration of the original atmosphere is one of the main aims of the conservation program (Vouvé et al. 1983).

From 1958 to 1963, a mechanical forced-air system was installed in the machine room for regulating the cave environment to account for the increasing number of tourists. The result was a system designed to adapt the subterranean climate of the cave to the visits.

Figure 7a, b
Cartography of the evolution of the condensation droplets on the horizontal vault of an archaeological site shown (a) on 25 March 1992 and (b) on 28 March 1992.

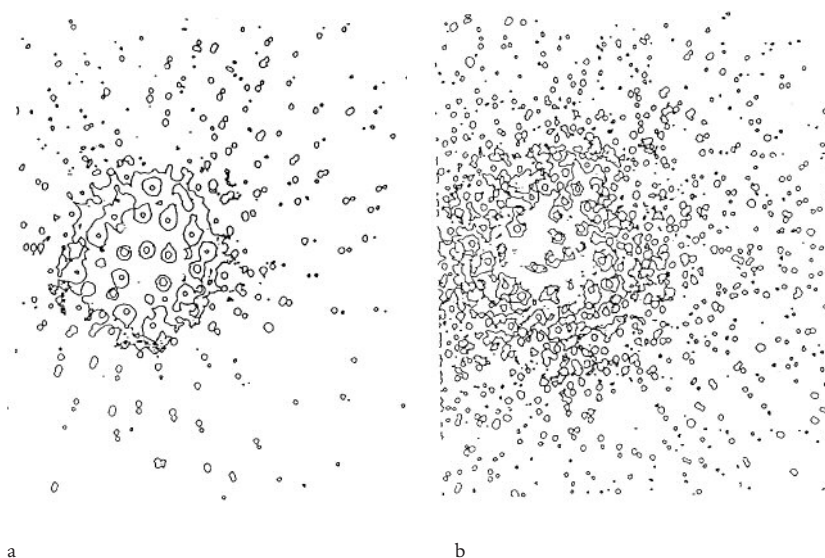
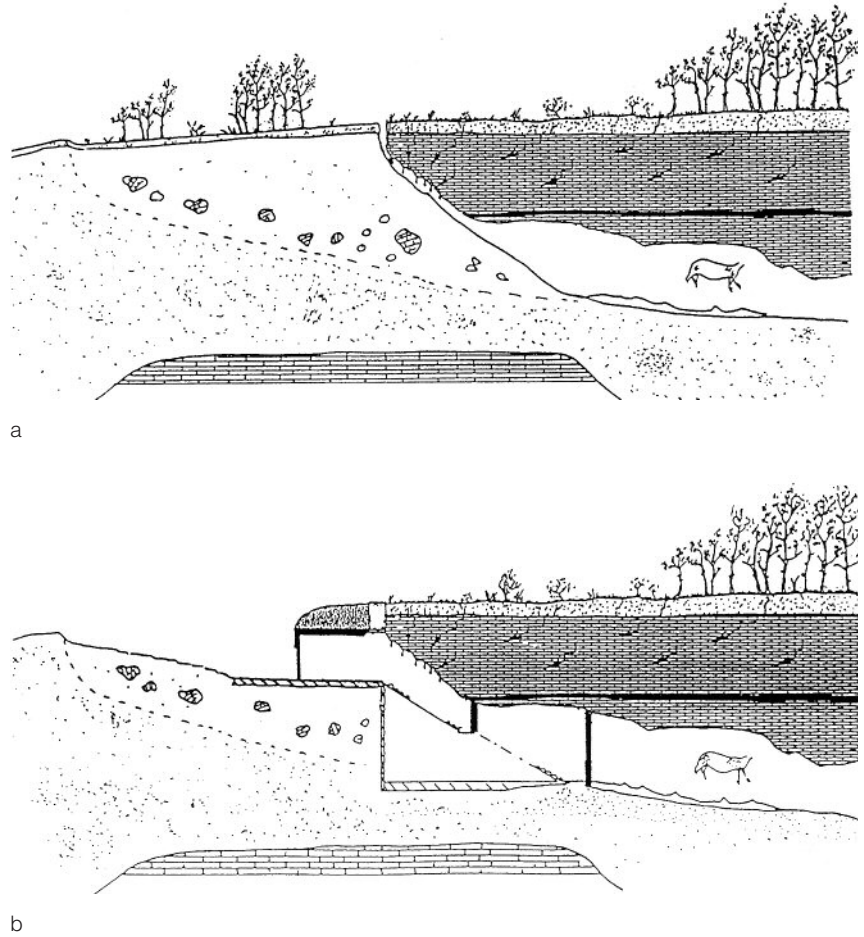


Figure 8a, b

State of the access of Lascaux (a) in 1940, the year of its discovery; and (b) in 1963.



Extensive scientific study preceded the installation of the regulating equipment (Malaurent, Vouvé, and Brunet 1992:319–32). The research monitored the following parameters (Fig. 9):

- Temperature of the air inside the cave at twenty-four specific points
- Temperature of the rock inside the cave at nineteen specific points
- Readings of the maximum and minimum external temperatures, and rainfall data from a meteorological station
- Assessment of the development of water from the phreatic water table intercepted by the entrance porch
- Assessment of the temperature at the intake and outlet vents of the primary cooling system
- Assessment of the temperature at the intake and outlet vents of the two secondary cooling systems
- Regulation of the output of the primary and secondary cooling systems
- Readings of air and water-vapor pressure taken with psychrometers from several strategic points within the cave
- Readings of CO₂ content in the enclosed spaces and pits

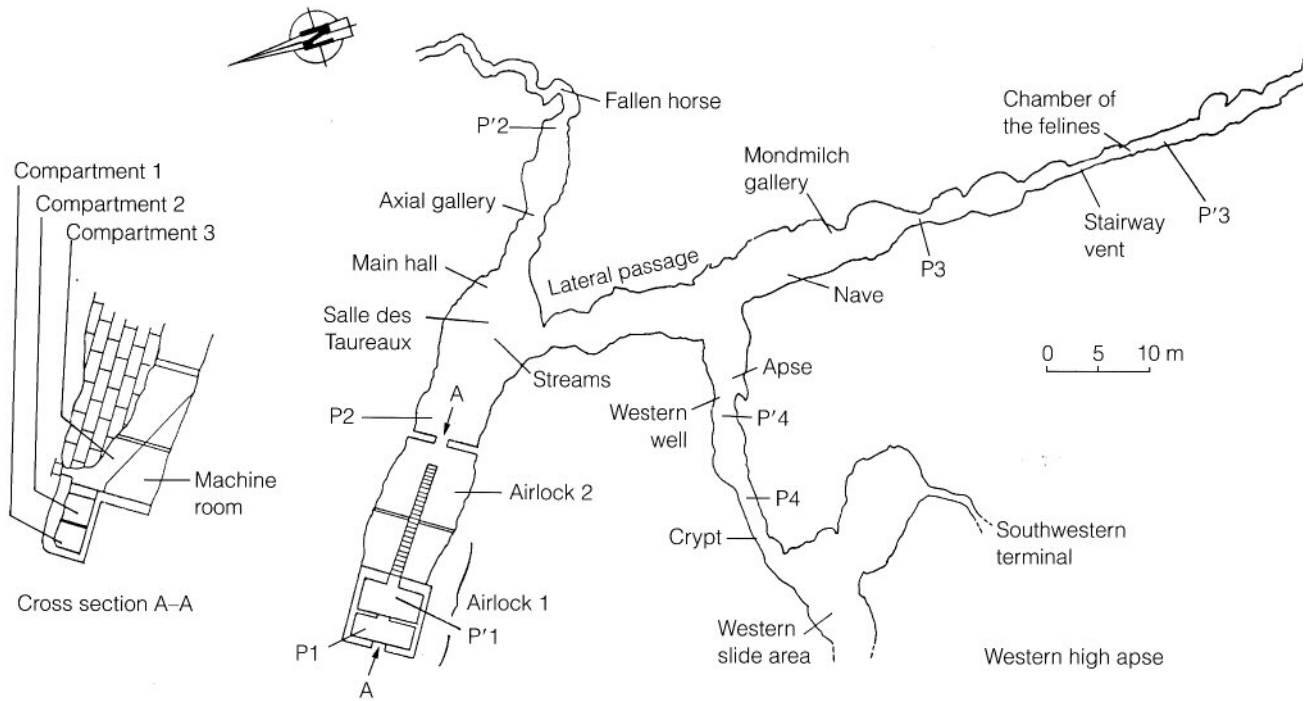


Figure 9
Map of Lascaux cave with main points where measurements were taken.

- Visual assessment of condensation on sensitive surface areas inside the cave
- Visual assessment of all the decorated surfaces
- Photographic assessment of pinpointed trouble spots



Figure 10
Painting in the Salle des Taureaux, Lascaux, showing an animal drawn on limestone and concretion.

The air-conditioning system has two closed circuits: circuit A (at a temperature of 5 °C), linked with the external cooling units; and circuit B (at 7 °C), which is internal. These two circuits are connected by exchanger D (Fig. 13). Exchangers C provide negative kilocalories (cold) from about June to December. Thus, controlling seasonal variations caused by the removal of part of the original screen, which acted as a natural exchange regulator between the Salle des Taureaux and the central branch of the cave, resulted in relatively good conservation conditions for the paintings (Fig. 9).

Monitoring of the rock in the Salle des Taureaux (chamber of the bulls) has demonstrated the need to control seasonal factors. Because of the slow progression of thermal waves in the ground during the winter period, the rock in this area is influenced by the air coming from more exposed areas, such as the machine room, which is closer to the exterior. Cooling air circulating from the cave’s vault network to the top openings in the machine room produces water condensation (from one to several liters of water per day) on the radiators (the coldest points in the system). The cooled air, which is now drier, then returns to the decorated vault network via the bottom openings in the machine room (Fig. 13).

In June, the cave generally appears to be in a stable condition, and the temperature of the rock surface begins to fall naturally with the onset of winter. However, the premise is that the water-vapor level in the



Figure 11
"Chinese horse" drawn on cauliflower deposit.

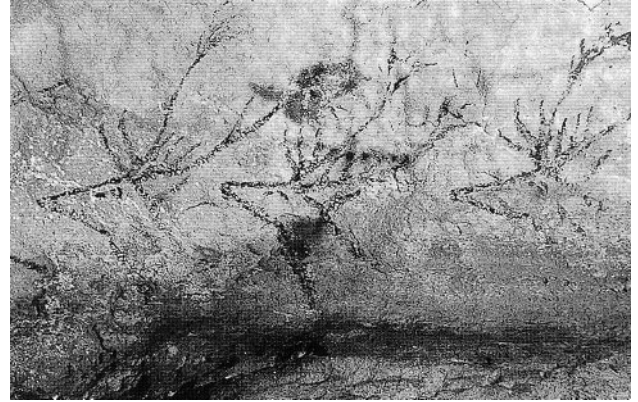


Figure 12
Frieze of deer drawn on limestone.

machine room air is higher than in the Salle des Taureaux. In order to avoid any condensation on painted walls, the cooling system is turned on. This helps stabilize the water-vapor pressure of the air and prevents condensation on the walls (Fig. 14).

Figure 13
Lascaux, simplified diagram of the air circulation in the cave. The cross section shows the accelerated convection controlled by machinery between the Salle des Taureaux and the machine room. Scale drawing showing the dynamic of airflow in the rooms and corridors: A = primary cooling system; B = secondary cooling system; C = thermic exchangers; D = cylindrical thermal exchanger; E = infiltration water; F = air circulation by natural convection.

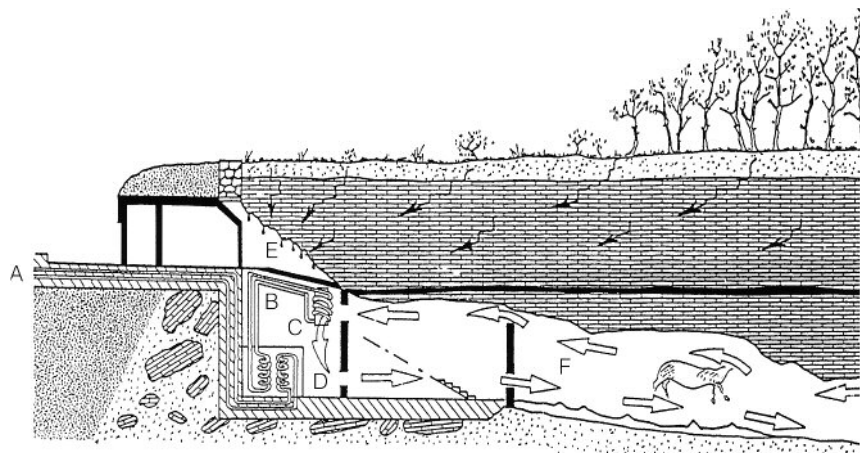
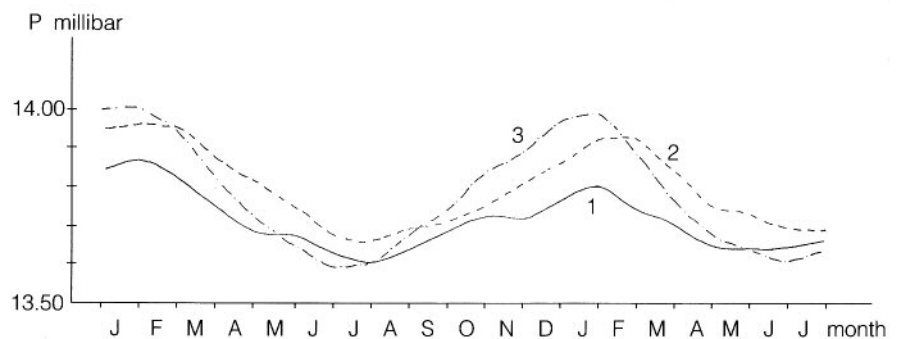


Figure 14
Diagram showing the pressure of water vapor expressed in millibars in the Salle des Taureaux: curve 1 = partial pressure of water vapor in the air; curve 2 = partial pressure of the counterbalancing water vapor of the surface of the rock on the left-hand wall; curve 3 = partial pressure of the counterbalancing water vapor of the rock on the vault. A comparison of curves 1 and 2 shows that there is no possibility of water vapor condensing, for example, on the rock near the drawing called "Unicorn."



Conclusions

Like any cave system, the Lascaux caves are a complex, living environment where different physical, chemical, and biological processes are constantly taking place and are subject, with a delayed effect, to external influences transmitted through rock, water, and air. The cave paintings are affected by the thermal, hydrous, chemical, and biochemical exchanges between rock and air.

Studies have revealed the relationship of this cave site to its environment; they have clearly shown that the equilibrium reestablished after all the changes the caves have undergone since their discovery in 1940 is of an extremely delicate nature.

The best possible conditions for the conservation of paintings have been achieved as a result of the smooth functioning and maintenance of the mechanical equipment. This is used to regulate the temperature of the caves through the operation of heat exchangers.

For Lascaux, as for other archaeological sites where wall paintings or drawings have finally been brought into a state of equilibrium with the environmental conditions, the authors agree with Mora, Mora, and Philippot (1977). These authors find that the best solution is to ensure conservation in situ by means of an overall air-conditioning system designed either to maintain the original conditions or to modify them very gradually, if and when necessary, under very close supervision.

Scientific conservation of cave sites depends largely on the ability to predict climatic and atmospheric changes, an ability that is grounded in knowledge of the changeable nature of the atmosphere. This understanding is essential in designing a conservation strategy that takes these parameters into account along with the need to obtain information concerning them as quickly as possible through the monitoring of both normal conditions and exceptional phenomena. Conservation professionals now have access to sophisticated equipment, such as reliable, battery-operated, high-performance telemeasuring units that, apart from being versatile, adapt to their environment and transmit information about it. Thus, it is now possible to control, organize, and influence most historic monuments at will, be they aboveground, half buried, or subterranean.

Acknowledgments

The authors wish to thank the Getty Conservation Institute, the Dunhuang Academy, and the National Chinese Institute of Cultural Property, who organized the conference; and Neville Agnew for his review of and comments on this article.

References

- Malaurent, P., J. Vouvé, and J. Brunet
 1992 Caractéristiques génétiques et conservatoires du climat souterrain en milieu karstique: Essai de restitution d'un paléo-faciès thermique, grotte de Lascaux. In *Karst et évolutions climatiques: Hommage à Jean Nicod*, 319–32. Talence: Presses Universitaires de Bordeaux.

- 1993 Les phénomènes d'évapocondensation et la conservation des milieux souterrains naturels et artificiels (décors et vestiges archéologiques): Approche théorique. In *Preprints of the 10th Triennial Meeting of the International Council of Museums (ICOM) Committee for Conservation, Washington, D.C., 22–27 August 1993*, ed. Janet Bridgland, 848–52. Paris: ICOM.
- Mora, P., L. Mora, and P. Philippot**
- 1977 *La conservation des peintures murales*. Bologna: Compositori.
- Schoeller, H.**
- 1972 Conduite de l'étude hydrogéologique et géologique des grottes descendantes. In *Congrès National de Spéléologie de Bordeaux*. Spelunca: Actes 7, 76–93.
- Stefanaggi, M., J. Vouvé, and I. Dargas**
- 1986 Climatic, hydrogeological and scientific study of the wall paintings of the crypt of Saint Savin sur Gartempe (Vienne, France). In *Case studies in the Conservation of Stone and Wall Paintings: Preprints of the Contributions to the Bologna International Institute for the Conservation of Historic and Artistic Works (IIC) Congress, 21–26 September, 1986*, 96–100. Bologna: Fondazione Internazionale Cesare Gnudi.
- Vouvé, J., J. Brunet, P. Vidal, and J. Marsal**
- 1983 Les oeuvres rupestres de Lascaux (Montignac, France): Maintien des conditions de conservation. *Studies in Conservation* 28(3):107–16.

Deposition of Atmospheric Particles within the Yungang Grottoes

Christos S. Christoforou, Lynn G. Salmon, and Glen R. Cass

ARCHAEOLOGICAL SITES, especially those exposed to nature's elements, degrade with time. This is due to physical, chemical, or biological erosion. Air pollution, wind-borne dust, and weathering by the elements over time can be significant factors. One such site is the Yungang grottoes in China. These grottoes are a collection of more than twenty cave temples, hollowed out of a sandstone cliff at Yungang, near the industrial city of Datong in northern Shanxi province. The work at Yungang was initiated under the supervision of the monk Tan-yao in 460 C.E., supported by the patronage of the Northern Wei dynasty. The five earliest caves were excavated in memory of the ruling monarch and his four predecessors. A number of lesser caves and niches were excavated during the early part of the sixth century (Cox 1957; Sickman and Soper 1968; Knauer 1983).

Most of the larger caves are similar in architecture, with rectangular rooms 10–15 m on each side, excavated around a central pillar that stretches from the floor of the cave nearly to the ceiling. Usually, the pillar is carved into a monumental statue of the Buddha. There are examples, such as Cave 6, where the central column is sculpted in the form of a pagoda. The caves usually have two openings to the outside: an entrance at ground level, and a window higher up at about the third-floor level. The interior walls of the caves are adorned with many sculptures and carvings that depict scenes from the life of the Buddha. Many of these carvings are still polychromed.

In antiquity, a wooden temple building one room deep was added to the front of each cave, as can be seen today only in front of Caves 5 and 6. According to reports (Cox 1957), repairs to the caves were made during the eleventh and seventeenth centuries, but by the early twentieth century they had fallen into a state of neglect. In more recent years, repairs have been made to stabilize some of the sculptures, and the area around the grottoes has been turned into a park. During 1986, the caves were cleaned, and documentary photographs of the statues were taken. Today the Yungang grottoes are open to the public, and they receive hundreds of visitors daily.

Yungang is located in the middle of one of China's largest coal mining regions. Airborne particles are generated by the various processes at the mines. Trucks that carry the coal away from the mines travel on a highway located only a few hundred meters away from the entrance of the caves, and these trucks generate a considerable amount of airborne coal dust and road dust. Coal is also used for heating and cooking in the village of Yungang, as well as to fuel the trains that transport coal from the mines. Airborne particles also are generated by traffic on the unpaved dirt roads in the village of Yungang, located immediately adjacent to the grotto site. A seasonal source of dust is present, especially in the spring, when winds blow from the desert, carrying soil particles. As a result of all these factors, the grottoes suffer from a severe soiling problem.

During April 1991, the authors conducted an extensive air monitoring program at the Yungang grottoes. Some of the experiments performed over the period of 12 April to 1 May 1991 are as follows:

1. The mass concentration and chemical composition of airborne particles and some pollutant gases (SO_2 , NO_2 , NH_3 , HNO_3 , HCl) were measured both outdoors and inside Caves 6 and 9. These measurements help to define how much dust and smoke is present in the outdoor air, and what fraction of that material is found inside the caves. Cave 6 retains its traditional wooden temple front building, while Cave 9 is open directly to the outdoor environment. One purpose of examination of these two sites was to measure the protective effect, if any, provided by the temple structure in front of Cave 6.
2. The size distribution of the airborne particles was measured both outside and inside Caves 6 and 9. This particle-size information was needed to support the design calculations for airborne particle-control systems, because the efficiency of particle filtration equipment depends heavily on adaptation to particle size.
3. The particle deposition flux onto both horizontal and vertical surfaces was measured outside and inside Caves 6 and 9. This allowed deposition rates measured during the 1991 experiments to be compared to historically observed particle accumulation rates on the statues. It also quantified the actual problem that this work was intending to control.
4. The air exchange that transports outdoor airborne particles into the caves was measured, along with indoor-outdoor pressure differences and the cave wall-air temperature differences that cause this air exchange.

In addition, the staff at the Yungang grottoes operated air-sampling equipment and measured airflow into and out of Caves 6 and 9 during the months of July and October 1991 and January 1992. This extended experiment, when combined with the April experiments, permitted a full annual cycle of conditions at the grottoes to be examined.

Experimental Methods

Many of the experimental methods used at the Yungang grottoes were essentially the same as the procedures that the authors have developed for examination of particle deposition and soiling problems inside Southern California museums, under the sponsorship of the Getty Conservation Institute (Nazaroff et al. 1990; Nazaroff et al. 1992, 1993; Ligocki et al. 1993).

Sampling equipment was placed outside Cave 9, under the protective overhang of the cliff above, and inside both Caves 6 and 9, at locations shown in Figures 1 and 2. Horizontally and vertically oriented deposition plates for dust collection were placed both outside and inside the caves, as shown in these figures. Airborne particle-mass concentration was measured by collection on membrane filters, followed by chemical analysis for carbon particles, ionic species—including sulfates, nitrates, chlorides, and ammonium ion—and trace metals from which soil-dust mineralogy can be studied. Pollutant gases were measured by collection on chemically treated backup filters, located downstream of filters used for particle collection.

Figure 1
Location of ambient atmospheric particle samplers, deposition plates, and sites (numbered) at which historically accumulated particle deposits were measured in Cave 9 at the Yungang grottoes (from Christoforou, Salmon, and Cass 1994).

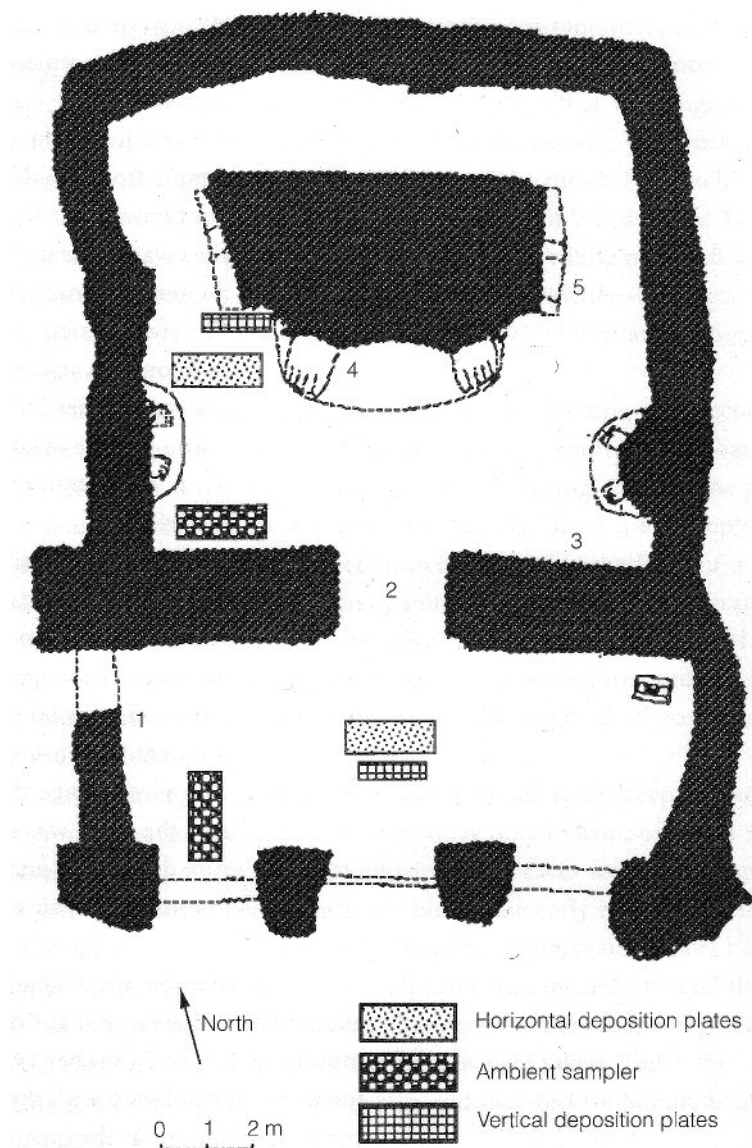
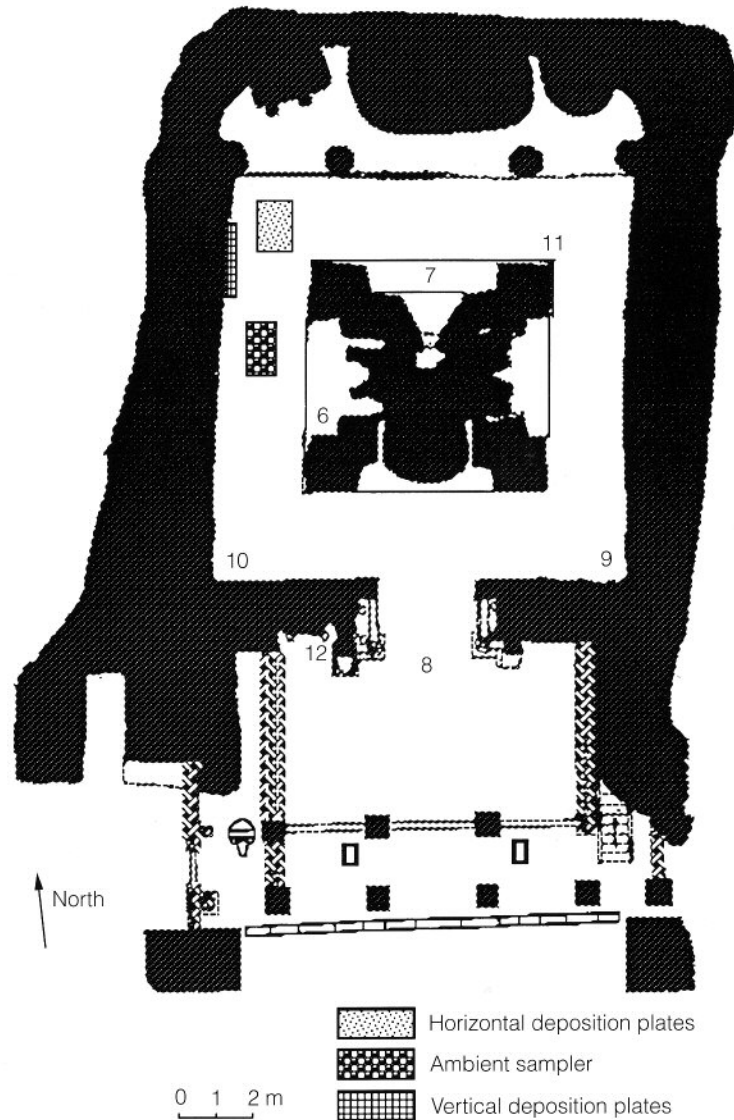


Figure 2

Location of ambient atmospheric particle samplers, deposition plates, and sites (numbered) at which historically accumulated particle deposits were measured in Cave 6 at the Yungang grottoes (from Christoforou, Salmon, and Cass 1994).



The size distribution of airborne particles was measured by computer-controlled, automated light microscope analysis of samples collected on membrane filters, while the size distribution of particles deposited on surfaces was measured by the same method applied to glass microscope slides that were used as deposition collectors in the caves. A complete description of experimental and analytical methods is given in the original technical reports on this work (Christoforou, Salmon, and Cass 1994; Salmon, Christoforou, and Cass 1994).

Airborne Particle Concentrations

The annual average concentration and chemical composition of outdoor airborne particles at Yungang is shown in Figures 3 and 4, from data contained in Salmon, Christoforou, and Cass (1994). The coarse particles examined in Figure 3 are large dust particles (diameter greater than $2.1 \mu\text{m}$) that settle out of the atmosphere easily, while the fine particles (diameter less than $2.1 \mu\text{m}$) examined in Figure 4 are the size of those in cigarette smoke and follow the air flow without depositing easily.

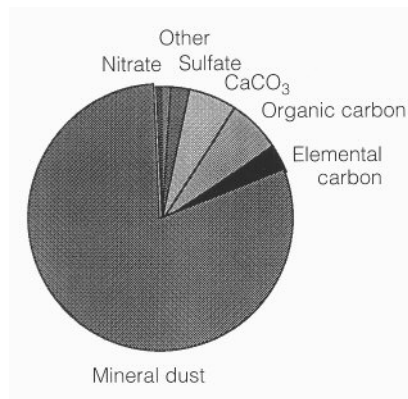


Figure 3
Chemical composition of coarse airborne particles (diameter $> 2.1 \mu\text{m}$) measured outdoors at the Yungang grottoes, 1991–92. The annual average coarse-particle concentration is $378 \mu\text{g m}^{-3}$. Coarse particles are about 80% mineral dust plus about 10% carbon particles (e.g., coal).

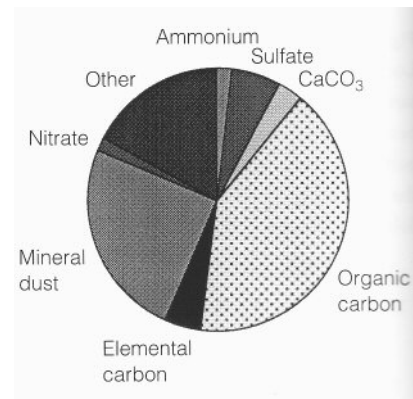


Figure 4
Chemical composition of fine airborne particles (diameter $< 2.1 \mu\text{m}$) measured outdoors at the Yungang grottoes, 1991–92. The annual average fine-particle concentration is $130 \mu\text{g m}^{-3}$. Fine particles are about 46% carbon plus about 24% mineral dust.

Annual coarse-particle concentrations outdoors during 1991–92 averaged $378 \mu\text{g m}^{-3}$, increasing to more than $1,200 \mu\text{g m}^{-3}$ during peak twenty-four-hour sampling periods. These coarse-particle concentrations are quite high, about six times higher than in the middle of the city of Los Angeles, California. The coarse particles consist largely of mineral dust, accounting for over 80% of the coarse-particle-mass concentration. Carbon-containing particles (organic compounds plus black elemental carbon) account for an additional 10% of coarse-particle mass.

Airborne fine-particle concentrations outdoors averaged $130 \mu\text{g m}^{-3}$. That is about four times higher than in the center of downtown Los Angeles, a location generally thought to be quite high in fine particles. These very small particles consist of carbon-containing particles (46%), followed in importance by mineral dust (crustal, 24%).

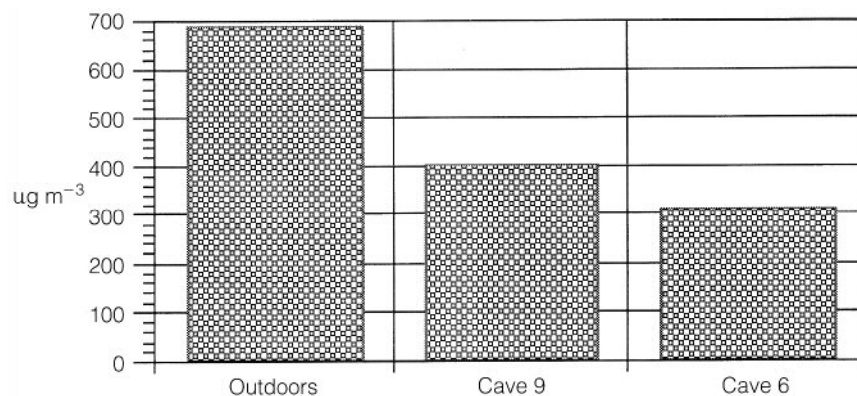
Figure 5 shows airborne particle concentrations during April 1991, when samples were taken outside and inside both Caves 6 and 9. Concentrations inside Cave 9 are lower than outside but higher than in Cave 6. Cave 9 receives air directly from outside because there is no wooden temple front building to provide particle removal or protection, as in the case of Cave 6. The concentrations inside Cave 9 are lower than outside, probably because of particle removal by deposition onto surfaces inside the cave, as there is no other mechanism for particle removal at this cave.

Dust Deposits in the Caves

The rate of accumulation of deposited particles on upward-facing surfaces was measured over a one-year period (Christoforou, Salmon, and Cass 1994). The annual average mass deposition rate to horizontal surfaces was $13.4 \mu\text{g m}^{-2} \text{s}^{-1}$ outside and $5.2 \mu\text{g m}^{-2} \text{s}^{-1}$ inside Cave 6, as shown in Table 1. During April 1991, particle deposition measurements were made in Cave 9 and were found to be halfway between the mass flux measured outdoors and that measured in Cave 6. Historical accumulations of dust

Figure 5

Airborne particle concentrations measured outdoors, inside Cave 9, and inside Cave 6 during April 1991, showing the extent of protection provided by the present temple building in front of Cave 6, as compared to Cave 9, which lacks a structure.



were removed from measured areas in Caves 6 and 9 at the numbered locations shown in Figures 1 and 2, which are known to have been cleaned in 1986 (Christoforou, Salmon, and Cass 1994). Indoor deposit depths that accumulated on horizontal surfaces over that five-year period (1986–91) range from 0.1 to 0.8 cm, with mass accumulations up to 5 kg m⁻², as shown in Table 2. In Table 3, it is seen that the particle deposition rates measured during the 1991–92 experiments, if extrapolated to a five-year estimate, are within about a factor of two of the historically observed rate of particle accumulation. This suggests that our data provide a reasonable basis for testing the likely long-term effect of various particle deposition–control proposals.

Dust deposits removed from surfaces in the caves at locations shown in Figures 1 and 2 have been examined by optical microscopy and have been analyzed chemically by neutron activation analysis, by low-temperature ashing, and by X-ray diffraction (XRD). Dust deposits analyzed by optical microscopy show that the deposits consist of quartz (typically 14–44%) and feldspar (typically 14–30%), clay and other polycrystalline materials (typically 10–22%), and unburned coal dust (15–40%), plus a few

Table 1 Mass flux of particles deposited onto horizontal surfaces at Yungang, measured on glass deposition plates (from Christoforou, Salmon, and Cass 1994)

Location	Date	Mass flux (mg m ⁻² s ⁻¹)
Outdoors	April 1991	21.5
Cave 9	April 1991	13.4
Cave 6	April 1991	4.5
Outdoors	July 1991	12.7
Cave 6	July 1991	5.4
Outdoors	October 1991	7.2
Cave 6	October 1991	5.8
Outdoors	January 1992	12.3
Cave 6	January 1992	5.1
Outdoors	Annual average	13.4
Cave 6	Annual average	5.2

Table 2 Measurements of historical particle deposits accumulated on the sculptures in Caves 6 and 9 over the period of 1986–91. Measurements that were made at the locations in Caves 6 and 9 are shown in Figures 1 and 2 (from Christoforou, Salmon, and Cass 1994)

Site	Location	Depth (cm)	Mass (g m^{-2})
Outdoors	1	0.76	6658
Cave 9	2	0.25	2695
Cave 9	4	0.13	572
Cave 9	5	0.80	4981
Cave 6	6	0.13	201
Cave 6	7	0.06	113
Cave 6	9	0.50	156
Cave 6	10	0.40	171
Cave 6	11	0.50	298
Cave 6	12	0.10	370

Table 3 Comparison of particle mass accumulated during the period of 1986–91 compared to that of the five-year estimate from the 1991–92 deposition experiments

Location	1986–1991 Actual, g m^{-2}	Five-year estimate from glass plate samples, g m^{-2}
Inside Cave 6	113–370	716
Inside Cave 9	572–4981	2113
Under cliff overhang in front of Cave 9	6658	3390

percent calcite. Low-temperature ashing likewise suggests that the dust deposits contain 18–32% coal dust. That the deposits are composed of a mixture of soil dust and coal dust is quite consistent with the nature of the pollution sources nearest to the caves.

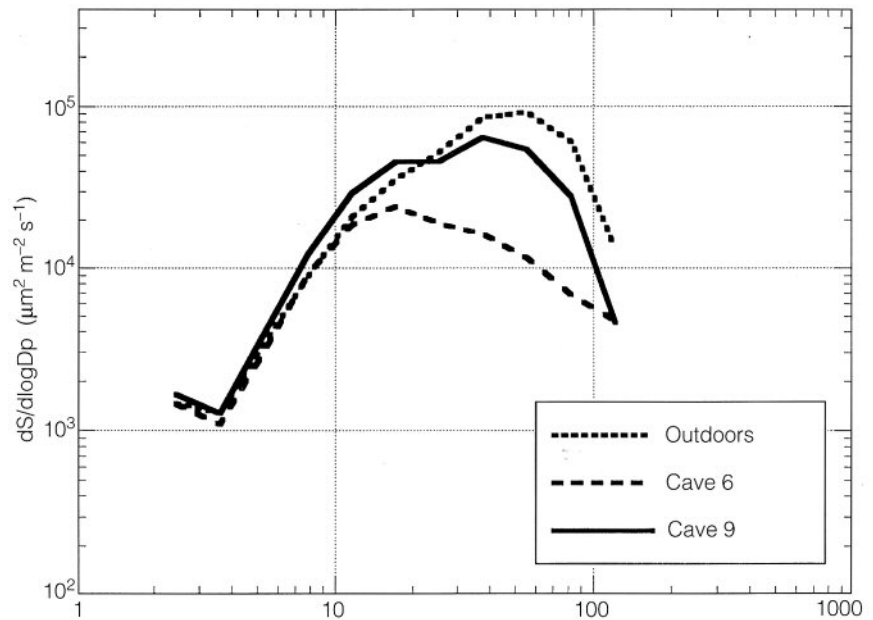
The rate of surface area coverage by coarse particles on horizontal surfaces inside the caves is very rapid (Fig. 6). More than 0.2% of the horizontal surface area in Cave 6 is covered by newly deposited particles in less than two hours. This means that a human observer looking at a new sheet of white paper placed in the caves could detect visually that the paper was becoming soiled within a matter of hours (Hancock, Esmen, and Furber 1976). Fortunately, the particles that produce this soiling problem are rather large (as shown in Fig. 6), in the size range of 10 to 100 μm in diameter. Particles of that size are relatively easy to remove by filtration of the air entering the caves.

Conclusions

Airborne particle concentrations and deposition rates have been measured both inside and outside the Buddhist cave temples at Yungang. The outdoor particle concentrations were very high. Total particle concentrations averaged 508 $\mu\text{g m}^{-3}$ over the year studied (1991–92), with 378 μg

Figure 6

Rate at which a horizontal surface at Yungang is covered by deposited particles as a function of particle diameter.



m^{-3} of that particle concentration present as coarse particles (diameter greater than $2.1 \mu\text{m}$), and $130 \mu\text{g m}^{-3}$ of that particle concentration present as fine particles (smaller than $2.1 \mu\text{m}$ particle diameter).

Chemical analysis has shown that the airborne particles consist mostly of mineral dust (24% and 80% for fine and coarse particles, respectively) and carbon particles (46% and 10% for fine and coarse particles, respectively).

The deposition rate of coarse particles onto upward-facing horizontal surfaces also was measured. At the deposition coverage rate of $2.9 \times 10^5 \mu\text{m}^2 \text{m}^{-2} \text{s}^{-1}$, observed during the spring of 1991 within Cave 9, horizontal surfaces would reach 0.2% coverage—the minimum percentage for detectable soiling (Hancock, Esmen, and Furber 1976)—in about $6.9 \times 10^3 \text{ s}$ or 1.9 h (on average). This example is completely consistent with the authors' observations that the glass plates and millipore filters used as deposition collectors in these experiments were noticeably dirty at the end of a day. At such deposition rates, complete coverage of the horizontal surfaces in the caves by a monolayer of deposited particles would occur within 1.3 months. Over a period of six years, deposits as deep as 0.8 cm and weighing as much as 5 kg m^{-2} have been measured at sites known to have been cleaned in 1986.

Clearly, airborne particle concentrations and particle deposition rates are so high at present that, by continuously covering the statues with a layer of abrasive and dark-colored dust, they would defeat any attempt to restore the caves. Fortunately, the surface area coverage rate is dominated by particles between $10 \mu\text{m}$ and $100 \mu\text{m}$ in diameter, which can be filtered out of the air entering the caves fairly easily. In a subsequent chapter herein, the air-quality and particle-deposition data reported here are used to evaluate the likely effect of alternative approaches to control of the particle deposition problem at the Yungang grottoes (see Christoforou et al., herein).

Acknowledgments

This work was supported by a research agreement from the Getty Conservation Institute. The cooperation and assistance of the staff of the Yungang grottoes and the State Bureau of Cultural Relics are gratefully acknowledged, including Huang Kezhong, Zhu Changling, Sheng Weiwei, Li Xiu Qing, Li Hua Yuan, Xie Ting Fan, Yuan Jin Hu, Huang Ji Zhong, and Zhi Xia Bing. The authors also extend their thanks to Bo Guo Liang of the Shanxi Institute of Geological Science, and Zhong Ying Ying from Taiyuan University. Assistance critical to this work was provided by the Getty Conservation Institute and its consultants, and we especially thank Neville Agnew, Po-Ming Lin, Shin Maekawa, and Roland Tseng for their help. Analysis of the chemical composition of the particle deposit samples from the caves by X-ray diffraction and light microscopy was performed at R. J. Lee Group, Monroeville, Pennsylvania, under the direction of Gary Casuccio, Mike Leger, Carol Richardson, and Tracy Moore.

References

- Christoforou, C. S., L. G. Salmon, and G. R. Cass
1994 Deposition of atmospheric particles within the Buddhist cave temples at Yungang, China. *Atmospheric Environment* 28:2081–91.
- Cox, L. B.
1957 *The Buddhist Cave-Temples of Yun-Kang and Lung-Men*. Canberra, Australia: Australian National University.
- Hancock, R. P., N. A. Esmen, and C. P. Furber
1976 Visual response to dustiness. *Journal of the Air Pollution Control Association* 26:54–57.
- Knauer, E. R.
1983 The fifth century A.D. Buddhist cave temples at Yun-Kang, North China. *Expedition* (Summer): 27–47.
- Ligocki, M. P., L. G. Salmon, T. Fall, M. C. Jones, W. W. Nazaroff, and G. R. Cass
1993 Characteristics of airborne particles inside Southern California museums. *Atmospheric Environment* 27A:697–711.
- Nazaroff, W. W., M. P. Ligocki, T. Ma, and G. R. Cass
1990 Particle deposition in museums: Comparison of modeling and measurement results. *Aerosol Science and Technology* 13:332–48.
- Nazaroff, W. W., M. P. Ligocki, L. G. Salmon, G. R. Cass, T. Fall, M. C. Jones, H. I. H. Liu, and T. Ma
1992 *Protection of Works of Art from Soiling Due to Airborne Particles*. Getty Conservation Institute Scientific Program Report. Marina del Rey, Calif: Getty Conservation Institute.
- 1993 *Airborne Particles in Museums*. Research in Conservation series. Marina del Rey, Calif: Getty Conservation Institute.
- Salmon, L. G., C. S. Christoforou, and G. R. Cass
1994 Airborne pollutants in the Buddhist cave temples at the Yungang Grottoes, China. *Environmental Science and Technology* 28:805–11.
- Sickman, L., and A. Soper
1968 *The Art and Architecture of China*. Pelican History of Art. New Haven and London: Yale University Press.

Control of Particle Deposition within the Yungang Grottoes

Christos S. Christoforou, Lynn G. Salmon, Timothy J. Gerk, and Glen R. Cass

THE YUNGANG GROTTOES, located near Datong, China, consist of more than twenty cave temples that contain dozens of monumental Buddhist statues and more than fifty thousand smaller sculptures. The sculptures within the caves are soiled at a rapid rate by the deposition of airborne particles. During April and early May 1991, experiments were conducted at Yungang to measure the nature of this soiling problem. The purpose of the experiments was to collect data necessary for the selection of an approach that would greatly reduce the soiling rate inside the caves.

The results of those experiments, reported in the technical literature (Christoforou, Salmon, and Cass 1994; Salmon, Christoforou, and Cass 1994) and summarized by Christoforou, Salmon, and Cass herein, show that the outdoor airborne particle concentrations at Yungang are very high, averaging $508 \mu\text{g m}^{-3}$ over an annual period (1991–92). Deposition of particles, typically ranging in size from 10 to $100 \mu\text{m}$ in diameter, occurs on horizontal surfaces within the caves largely due to gravitational sedimentation. The result is that the horizontally oriented surfaces of the sculptures within the grottoes can become noticeably soiled within a matter of hours and can become completely covered by the first monolayer of deposited dust within 1.3 months. Over a period of six years, deposit thicknesses as deep as 0.8 cm and weighing as much as 5 kg m^{-2} have been measured on the statuary in the caves (see Christoforou, Salmon, and Cass herein).

Measurements of the chemical composition of the airborne particles and of the dust deposits on surfaces in the caves show that they consist of mineral matter (e.g., soil dust) and carbon particles (e.g., unburned coal dust) (Salmon, Christoforou, and Cass 1994; Christoforou, Salmon, and Cass herein). This is consistent with observations of the major dust generation activities in the vicinity of Yungang, which include emissions from large coal mines in the region; coal dust and road dust from trucks carrying coal (especially along a road located approximately 300 m to the south of the grottoes); dust from travel on unpaved roads in the village

of Yungang, adjacent to the grottoes; dust generated by visitors and maintenance activities on the unpaved terrace immediately in front of the caves; soil dust generated by wind storms from the Gobi Desert, and smoke from local coal combustion.

The purpose of this article is to examine alternative approaches to the control of the particle deposition problem within the Yungang grottoes. Two general approaches are possible: (1) control of particle concentrations in the outdoor air through reduction of particle generation at the aforementioned sources, and (2) removal of particles from the air entering the caves by filtration or similar technical means. Each of these alternatives is discussed in quantitative terms, based both on field experiments conducted at Yungang and on computer-based models of the particle deposition processes within the caves.

Control of Outdoor Pollutant Concentrations

A map of the immediate vicinity of the Yungang grottoes is shown in Figure 1. The cliff face into which the cave temples are excavated appears as an east-west line along the middle of the map. There is a park within the walls of the grotto grounds immediately to the south of the cliff face. The small village of Yungang lies directly to the south of the park in front of the caves. A major highway, carrying thousands of coal trucks daily, is located on the south and west sides of the village. A river runs past the grottoes site to the south and west of the coal-hauling highway. Just south and west of the river is a railroad line for coal-fired locomotives. Coal mines are sited at the periphery of the map, as well as up and down the river valley beyond the boundaries of what is shown in Figure 1.

Over a two-day period in April 1991, the authors measured the spatial distribution of the deposition of airborne particles at the center of a series of 0.5×0.5 km map sections laid out over the 2×2 km area surrounding the caves shown in Figure 1 (Salmon et al. 1995). Extra samples were collected within the village of Yungang and along the terrace in front of the caves. Measurements were made on glass deposition plates, and those results are shown in Figure 1. The highest deposition rates (about $60 \mu\text{g m}^{-2} \text{s}^{-1}$) occur in the center of the map, within the village of Yungang and along the coal-hauling highway. Lower particle fluxes generally occur at the edges of the area mapped. This means that the sources that generate much of the airborne particulate matter are located within the high-flux area, principally along the coal-hauling highway and inside the village of Yungang. The caves are located between the cleaner countryside and the very dusty area along the highway and the main street of the village. As a result, the particle deposition flux at the front of the caves is lower than that along the coal-hauling highway or in the village, but is higher than that in the surrounding countryside.

Because the area that seems to contain this high source of particles is fairly small, it may be practical to reduce much of the local particle generation by the following simple means: (1) redirecting the coal-truck traffic to roads located far from the grottoes or, alternatively, covering the loaded coal trucks so that coal does not fall off to be crushed and driven

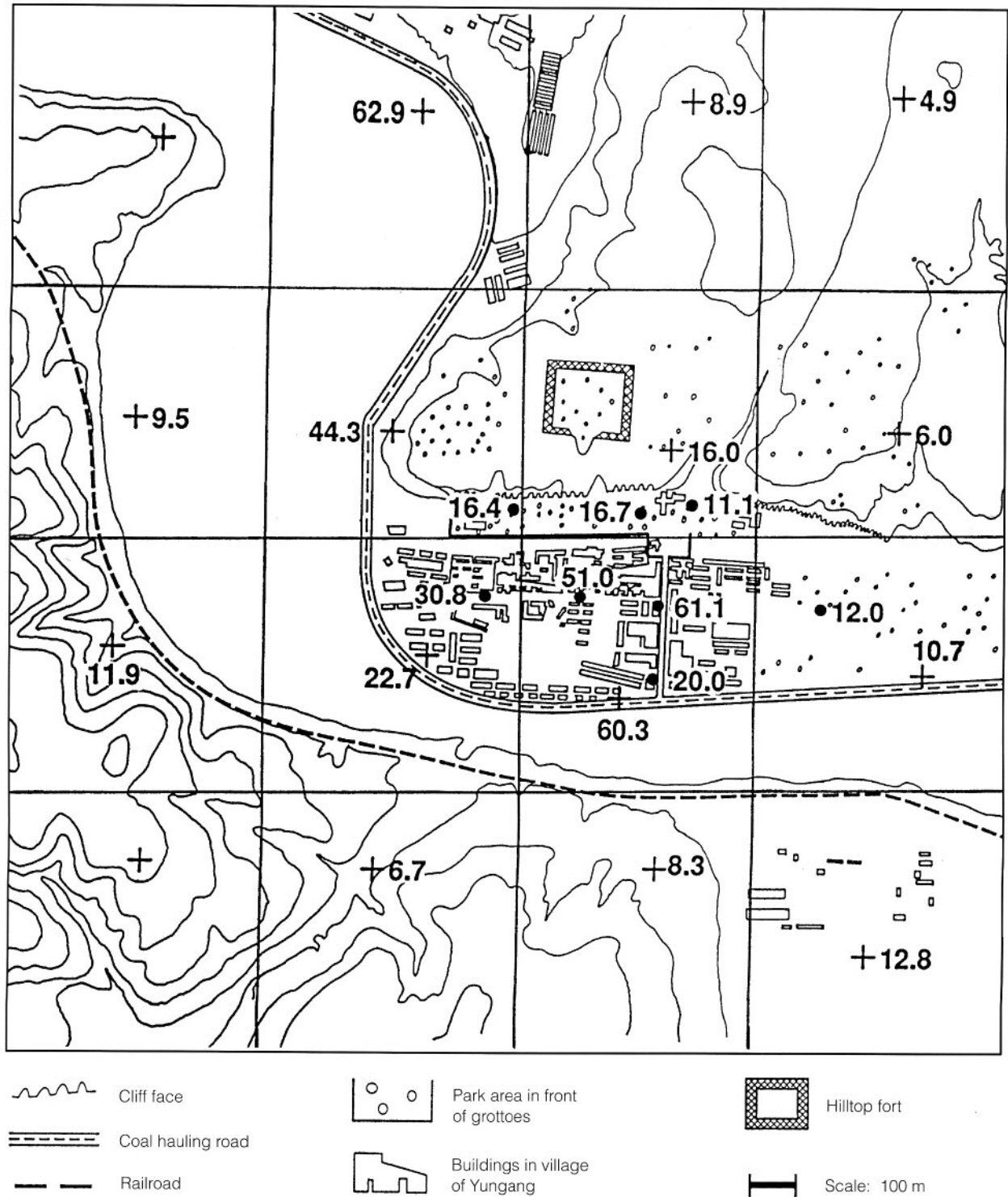


Figure 1 Map of the 2 x 2 km area surrounding the Yungang grottoes that was studied to determine the spatial distribution of the local particle deposition problem. Values shown at the experimental sites marked by + or • are airborne particle deposition rates in $\mu\text{g m}^{-2} \text{s}^{-1}$ measured over the period of 19–21 April 1991 (from Salmon et al. 1995).

into the air by trucks that follow; and (2) paving the few streets in the village of Yungang so that vehicle traffic produces much less dust there.

The authors have had occasion to observe that the city of Xian employs an excellent additional measure for dust suppression: a tank truck uses water to spray down the roads in the morning. This may, at first, seem impractical at Yungang, given the obvious general shortage of water in the area. But it should be seriously considered, as it is a measure that

the grottoes staff could undertake on their own initiative with little required assistance or cooperation from others. The sections of road to be washed (i.e., the section of the highway on the map of Figure 1, plus the village roads) are very short. The grottoes do have their own water source, but that water may not have to be used. There is no reason to wash the roads with high-quality water when a tank truck can fill up at the river (as long as the river is not dry). If necessary, a well could be drilled to increase the supply of locally available water.

A further source of possible dust creation is foot traffic and sweeping activity that occurs on the dirt terrace directly in front of the caves. Much of the dust deposited within the caves has a mineral composition similar to that of local soil dust. It is not easy to tell how much of this dust comes from the terrace in front of the caves and how much comes from the village. The Yungang grottoes staff has reported that there is a plan to pave the dirt area in front of the caves with stepping-stones, as a means of reducing dust generation at that site.

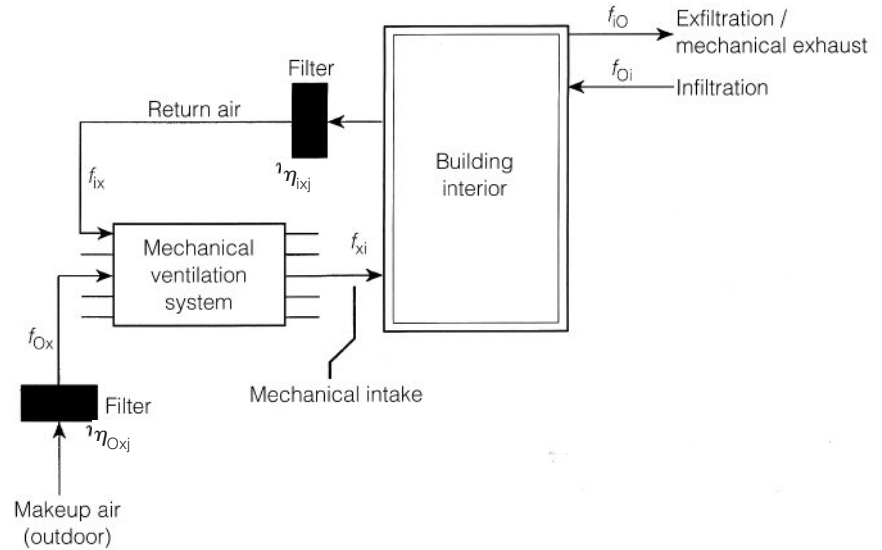
If localized particle generation from the coal-hauling highway, from the village, and from the dirt area just in front of the caves could be suppressed, particle deposition rates would begin to approach those in the areas of Figure 1 that are more distant from the caves. A reduction in particle deposition rates from about $16 \mu\text{g m}^{-2} \text{s}^{-1}$ at present at the entrance to the caves down to perhaps $10 \mu\text{g m}^{-2} \text{s}^{-1}$ in the future on days with conditions similar to those measured and shown in Figure 1 may be a reasonable goal. That would reduce particle deposition at the caves by about 38%. The reduction would not be larger because the regional background deposition rate all over the countryside—due to regionwide dust sources that include the coal mines, more distant road traffic, and other villages—is fairly high, even at sites distant from local dust sources that can be controlled, such as those near the village of Yungang. Thus, the use of local dust suppression methods at Yungang does not provide a complete solution to the particle deposition problem, but it helps. It may make an important contribution to an overall control program.

Removal of Particles from Air Entering the Grottoes

Two options exist for removing particles from the air that enters the grottoes. First, a mechanical air-filtration system, powered by an electrical fan motor, could be used. In antiquity, the entrance to each of the caves was sheltered by a wooden temple front building that was one room deep and extended several stories up the face of the cliff. Two of these structures still exist today. A mechanical air-filtration system could be concealed within the upper stories of an existing or reconstructed wooden temple front building. Many mechanical air-filtration systems are maintained in Beijing at present, only about 265 km to the west of Yungang; similar systems could be maintained at Yungang in the not-too-distant future. The second option would be a passive particle-filtration system that could be designed to make use of the natural convection-driven air circulation within the caves to remove particles as air passes through filter material. This filter material would replace the paper that originally covered the

Figure 2

Schematic representation of the mechanical air-filtration system for a building. The symbols f and η indicate airflow rates and filter efficiencies, respectively (from Nazaroff et al. 1993).



numerous windows that exist within the door panels of a traditional Chinese temple structure.

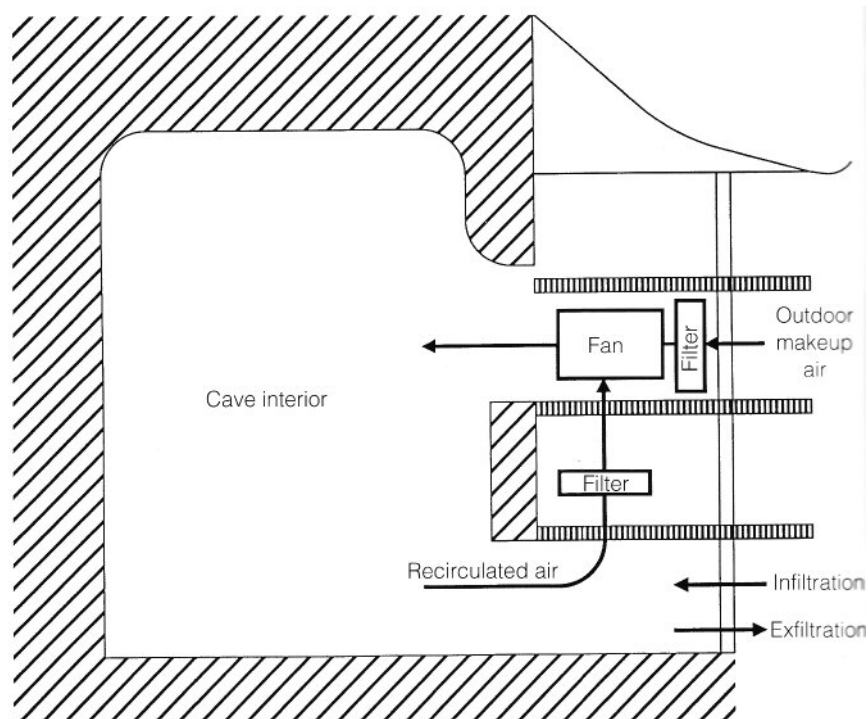
Installation of a mechanical air-filtration system

Figure 2 shows a diagram of a standard mechanical air-filtration system for a building. Outdoor makeup air containing airborne particles is fed to the ventilation system through a particle filter and is then introduced into the building (in this case a cave) interior. Previously filtered recirculated air is withdrawn from the building interior, filtered again, and then sent back to the building. This repeated filtration of the recirculated indoor air means that the removal efficiency of the whole system—defined as the percentage of the particles originally contained in air entering the building that are subsequently collected by the air-filtration system—is greater than it would be if the air made only one pass through the filters as it enters the building. A certain amount of infiltration air usually leaks, unfiltered, into the building through cracks or when doors are opened and closed.

A filtration system for Cave 6 at Yungang, for example, could be built by placing a mechanical fan, ductwork, and filters in a hidden, unused area of the upper stories of the wooden building that stands in front of that grotto. Such a system can be operated using many possible combinations of filters, outdoor makeup airflow rates, recirculated indoor airflow rates, and untreated outdoor air infiltration. The likely effects of different designs were explored. First, a computer model of the particle deposition process in Cave 6 was built as it would exist both with and without a wooden building in front, based on the calculation approach previously described by Nazaroff and Cass (1989) and Nazaroff, Salmon, and Cass (1990). Next, several alternative particle-filtration system designs were considered. A schematic diagram showing one possible relationship between equipment location and airflow pathways for such a system within a

Figure 3

Schematic diagram showing one possible relationship between equipment location and airflow for a mechanical air-filtration system concealed within the upper stories of a structure that shelters the front of a cave at Yungang.



Buddhist cave temple front structure is given in Figure 3. Finally, the change in particle deposition rates onto horizontal surfaces were calculated for several different ventilation system designs.

To begin this study, a base case condition was established at Cave 6 as it would exist if there were no temple building in front of the cave. This was an important case to consider because most of the other grottoes at Yungang lack a wooden building at present. The computer simulation began with measured outdoor particle concentrations and particle sizes observed on 15–16 April 1991, and then followed those particles as they entered the cave with the measured airflow. Under uncontrolled base case conditions, particle mass amounting to $262 \text{ mg m}^{-2} \text{ d}^{-1}$ was calculated to deposit on horizontal surfaces, as seen in line 1 of Table 1. In the presence of the existing wooden building in front of Cave 6, the flow of untreated outdoor air into the grotto is reduced from what it would be without the wooden building. In a simulation of the historical case at Cave 6 (which includes the effect of the existing wooden shelter in front of that cave), the particle flux to horizontal surfaces was equal to 53% of that for a cave with a completely unsheltered entrance (see line 2 in Table 1). The calculated particle deposition rate to horizontal surfaces in this second case compared closely with the measured particle deposition for the days studied, as seen in Figure 4.

Mechanical air-filtration systems in commercial buildings typically employ about a 1:3 ratio between filtered outdoor makeup air and recirculated, refiltered indoor air (Fig. 2). The effect of a standard ventilation system such as this can be approximated by setting the total airflow through such a system at $317 \text{ m}^3 \text{ min}^{-1}$ (identical to the natural airflow that would exist without a wooden building in front of Cave 6), with $89 \text{ m}^3 \text{ min}^{-1}$ of

Table 1 Effect of alternative mechanical filtration system designs on reducing the particle mass flux to horizontal surfaces in Cave 6 at the Yungang grottoes

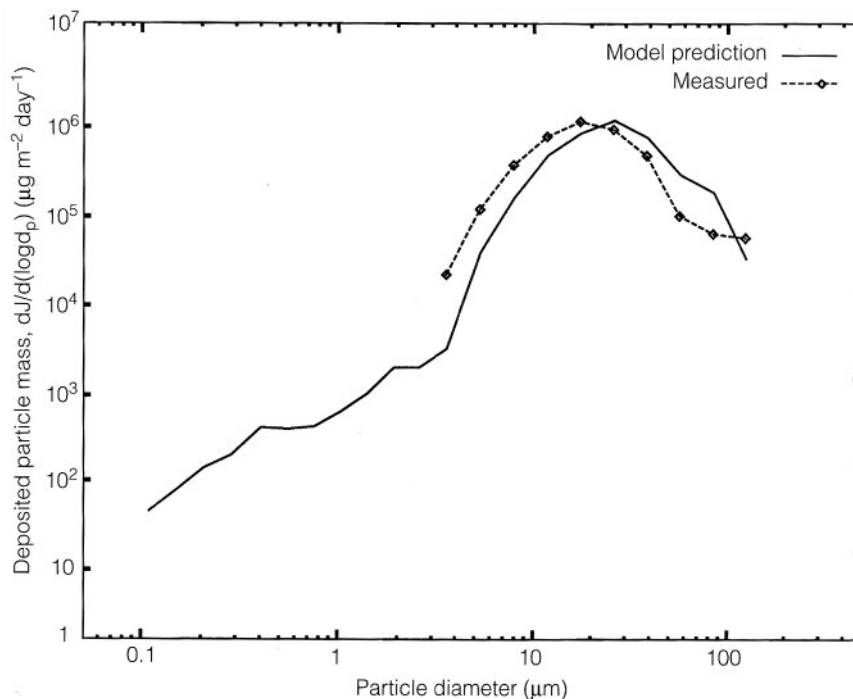
	Untreated outdoor infiltration air ($\text{m}^3 \text{min}^{-1}$)	Filtered outdoor makeup air ($\text{m}^3 \text{min}^{-1}$)	Filtered indoor recirculated air ($\text{m}^3 \text{min}^{-1}$)	Filter type	Mass deposition to horizontal surfaces ($\text{mg m}^{-2} \text{day}^{-1}$)	Percent remaining relative to base case	Time to 100% coverage by particles (years)
Base case							
(1) Temple front removed	317	—	—	—	262	—	0.28
(2) Historical case with wooden building	99	—	—	—	139	53	0.47
Mechanical ventilation with low-efficiency filters (F_{B1})							
(3) Standard system	10	89	267	FB1	92	35	0.75
(4) Reduced makeup air	10	22	334	FB1	37	14	1.8
(5) Standard system with zero infiltration	0.0	89	267	FB1	82	31	0.83
(6) Reduced makeup air with zero infiltration	0.0	22	334	FB1	24	9.2	2.6
Mechanical ventilation with loaded low-efficiency filters (F_{A3})							
(7) Standard system	10	89	267	FA3	12	4.6	5.7
(8) Reduced makeup air	10	22	334	FA3	9.9	3.8	7.2
(9) Standard system with zero infiltration	0.0	89	267	FA3	3.8	1.4	15
(10) Reduced makeup air with zero infiltration	0.0	22	334	FA3	1.5	0.6	36
Mechanical ventilation with high-efficiency filters							
(11) Standard system	10	89	267	88–99%	9.9	3.8	7.5
(12) Reduced makeup air	10	22	334	88–99%	9.4	3.6	8.0
(13) Standard system with zero infiltration	0.0	89	267	88–99%	1.5	0.6	42
(14) Reduced makeup air with zero infiltration	0.0	22	334	88–99%	0.93	0.4	72

Values shown are averages of model predictions over the two-day period of 15–16 April 1991, for which data are available to drive the deposition model. Deposition rates under annual average conditions are about four times higher than under 15–16 April 1991 conditions; deposition fluxes shown above should be scaled upward proportionately and the times to reach 100% coverage by particles should be divided by a factor of 4 when considering time periods that approach a year or longer.

outdoor makeup air and $267 \text{ m}^3 \text{min}^{-1}$ of recirculated indoor air. The infiltration of untreated air is set at $10 \text{ m}^3 \text{min}^{-1}$ (approximately 10% of the makeup airflow). In reality, this infiltration air will depend on how airtight the building is. The sum of outdoor makeup-air supply plus infiltration-air supply is identical to the $99 \text{ m}^3 \text{min}^{-1}$ outdoor air exchange rate observed historically in the presence of the existing wooden building in front of Cave 6, which is important from the point of view of water vapor removal. A separate study of the water vapor balance in Cave 6 is still needed to determine whether or not that historically observed air exchange rate is appropriate; the outdoor airflow could easily be increased if necessary. Initially, low-efficiency filters will be tried that have a single-pass particle removal efficiency of 14–34%, based on measurements made in a particular Southern California museum filtration system (see filter performance curve F_{B1} in Fig. 5, from Nazaroff et al. 1993). The result of such a system would be the reduction of particle deposition to 92 mg m^{-2}

Figure 4

Measured particle mass deposition rates onto horizontal surfaces as a function of particle size inside Cave 6 at Yungang, compared with model predictions of particle deposition rates based on outdoor particle concentration, particle size distribution, and airflow through the caves, observed on 15–16 April 1991. This is the base case model-verification-result that corresponds to line 2 of Table 1.

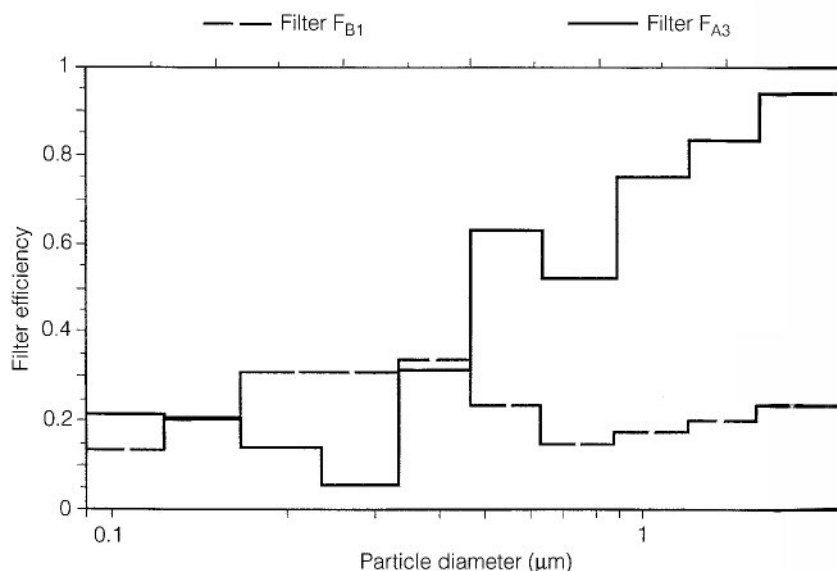


d^{-1} , or to 35% of the uncontrolled case, as seen in line 3 of Table 1. These filters were studied purely to illustrate the effect of changing the filtration efficiency. No recommendation of a particular filter manufacturer is intended at this point; that decision should be made later.

Further reduction in particle deposition can be attained by reducing the outdoor makeup air from $89 \text{ m}^3 \text{ min}^{-1}$ down to $22 \text{ m}^3 \text{ min}^{-1}$, while increasing the return airflow, thus bringing fewer new particles into the cave. The result of this change is shown on line 4 of Table 1. Particle deposition would be reduced to $37 \text{ mg m}^{-2} \text{ d}^{-1}$, or to 14% of the uncontrolled case. Though particle levels would be reduced, one must be careful

Figure 5

Filtration efficiency of particle filters as a function of particle size. The results are based on 21 hours and 4.5 hours of data for filters F_{A3} and F_{B1} , respectively. The corresponding operating flow velocities across the filter faces are 0.44 and 1.7 m s^{-1} . Filter media: Filter F_{A3} is Servodyne type SR-P1L; filter F_{B1} is Servodyne type Mark 80 (from Nazaroff et al. 1993).



to determine that the reduced air exchange rate does not lead to water vapor buildup in the cave.

No matter how good the filters are, the performance of the mechanical filtration system will be limited by the amount of untreated infiltration air that leaks into the building. The above two control cases have been rerun with zero untreated infiltration air, and the results are shown on lines 5 and 6 of Table 1. With the higher filtered outdoor make-up air supply, but no infiltration (line 5 of Table 1), particle mass deposition drops to 31% of the base case; with no infiltration air plus reduced makeup air, the particle deposition flux drops to 9.2% of the base case.

Further improvements can be made to the filtration system by using more efficient filters. One air-pass through filter F_{A3} (Fig. 5) removes about 96% of the very coarse dust particles that are causing much of the deposition problem in the caves. Filter F_{A3} has been used long enough that a “filter cake” of deposited particles has accumulated on its surface, making it harder for new particles to pass through the filter uncollected. This situation may be referred to as having a low-efficiency filter that is “loaded” with previously collected particles. The calculations performed in lines 3–6 of Table 1 are repeated for the case with the higher filtration efficiency of filter F_{A3} . Results are shown in Table 1, lines 7–10. The cases in lines 7 and 8 of Table 1 approach a situation in which about 4% of the particles in the outdoor air still remain, in spite of repeated passes through filters that are 96% effective per pass at removing coarse particles. This is occurring because unfiltered infiltration air is still entering. The purpose of the two cases on lines 9 and 10 of Table 1 is to illustrate the importance of eliminating untreated infiltration air. It may not be practical to completely eliminate infiltration, but it is important to try to do so. Relatively tight wood-frame buildings are constructed in the United States, so this requirement can even be met using traditional materials, if the structure is carefully designed.

A sequence of high-efficiency filters can be placed in the mechanical ventilation system to achieve 88% collection of fine particles and 95% (recirculated air line) to 99% (makeup air line) collection of coarse dust per pass. Such filters would cost more to operate because the pressure drop through the filters is higher, necessitating more power, a bigger fan, and more expensive filter material. In lines 11–14 of Table 1, the previous calculations are repeated for the case of the high-efficiency filters. The principal difference with the high-efficiency filters is that they reduce fine particle concentrations and thus will slow the rate of deposition onto the ceiling and vertical surfaces. The buildup of particles on vertical surfaces is already much slower than on horizontal surfaces. Before one can decide on the merits of the higher efficiency filters, it is important to know whether or not the horizontal surfaces of the statues (e.g., shoulders, tops of heads) will be cleaned separately and more frequently than the vertical surfaces (e.g., the chests of statues). If all surfaces are to be cleaned at the same time, then the horizontal surfaces will become dirty first and will trigger a round of cleaning regardless of whether filter F_{A3} or the more expensive high-efficiency filters are used. However, if one wants to clean

the vertical surfaces as infrequently as possible, the high-efficiency filters will make this possible.

Passive filtration systems

Given the large airflows through the caves caused by natural convection, the question arose: Is it possible to filter the particles out of the air entering the caves without using a mechanical fan to move the air? The authors approached this question by first building a computer-based model that calculated the changes in the natural convection-induced airflow through Cave 6 that would occur in response to obstructions to airflow presented by cracks and doors in the shell of the present wooden building in front of that cave. Then they calculated the airflow and particle removal that would occur if filter material were used in place of the paper windows in the door panels of the present structure in front of Cave 6, as shown schematically in Figure 6.

The first two lines of Table 2 are again the uncontrolled base case with no structure in front of the cave and the case where the cave operates as it is today, respectively. The next line in Table 2 shows the amount of control one would exercise if the doors at the ground level and the balcony doors and/or windows on the upper floors of the building in front of Cave 6 were kept closed at all times. Airflow in and out of the cave would then flow through the existing cracks around the door and window panels. Our model suggested that in this case the average flow of air into Cave 6 under the conditions of 15–16 April 1991 would be $26 \text{ m}^3 \text{ min}^{-1}$, as opposed to $99 \text{ m}^3 \text{ min}^{-1}$ for the cave as it is operated today with doors open during the day but closed at night and with several door panels left

Figure 6
Schematic diagram of a passive air-filtration system, showing placement of filter material in the outer wall panels of a shelter in front of a cave at Yungang.

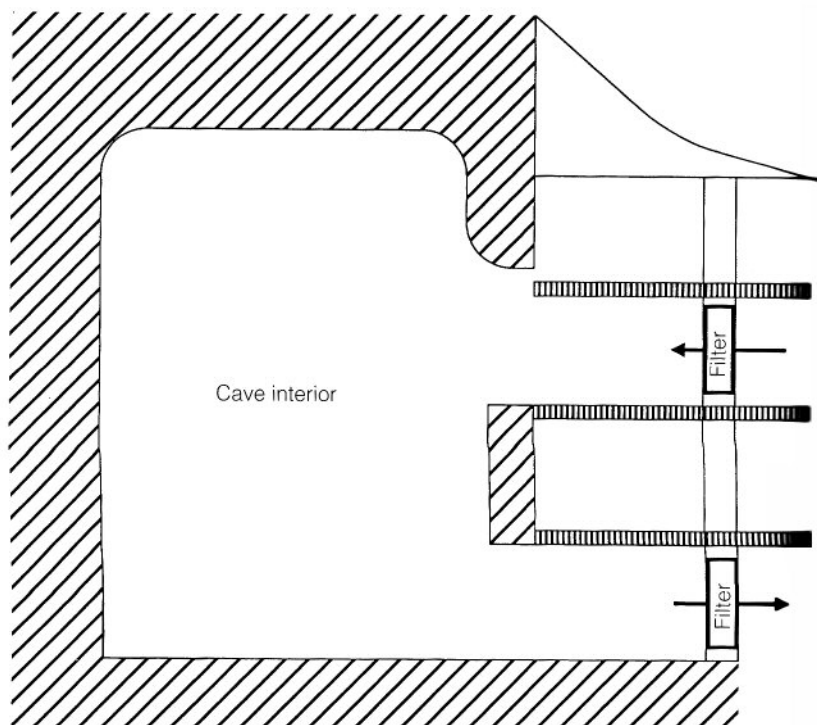


Table 2 Effect of alternative passive filtration system designs on reducing the particle mass flux to horizontal surfaces within a cave the size of Cave 6 at the Yungang grottoes^a

	Air flow through cave (m ³ min ⁻¹)	Mass deposition to horizontal surfaces (mg m ⁻² day ⁻¹)	Percent remaining relative to base case	Time to 100% coverage by particles (years)
Base case				
(1) Temple front removed	317	262	—	0.28
(2) Historical case with wooden building	99	139	53	0.47
Tightening up the wooden building				
(3) Closed doors ^b	26	50	19	1.0
Filter material installed in place of paper windows				
(4) Building still leaks ^{c,d}	34	45	17	1.2
(5) Building has no leaks ^{c,e}	6.3	3.4	1.3	9.0
Maximum amount of filter material installed				
(6) Building has no leaks ^f	86	7.5	2.9	6.3

^a Values shown are averages of model predictions over the two-day period of 15–16 April 1991, for which data are available to drive the deposition model. Deposition rates under annual average conditions are about four times higher than under 15–16 April 1991 conditions; deposition fluxes shown above should be scaled upward proportionately and the times to reach 100% coverage by particles should be divided by a factor of 4 when considering time periods that approach a year or longer.

^b The only control measure in this case is to ensure that the doors at the ground-floor level as well as balcony doors and windows on the upper floors remain closed at all times.

^c Filter material with low-pressure drop characteristics is installed on the available window panels on both the ground floor and the third floor in the place of the existing paper windows. The pressure drop and efficiency characteristics of Minnesota Mining and Manufacturing, Inc. filter type GSB-30 have been used in these calculations.

^d The doors on the ground floor as well as windows and balcony doors on the upper floors are assumed to remain closed at all times, but there is infiltration of air through cracks around the doors and windows of the building shell. Calculations show that 71% of the total mass of air that enters the cave does so through the cracks. Filter area both on the ground floor and the third floor level totals 2.56 m² at each level.

^e In this case the cracks in the building shell have been caulked and all air entering the cave must pass through the filter material. Filter area both on the ground floor and the third level totals 2.56 m² at each level.

^f Same as in Note e, except now the filter material has been increased: 55.4 m² filter surface area is supplied on the upper floors and 46.0 m² filter surface area on the ground floor. This is consistent with the filter surface area that could be incorporated into a new shelter in front of a cave, but exceeds the amount of filter surface area that can be incorporated into the historical wooden building in front of Cave 6.

open on the upper floors, and 317 m³ min⁻¹ for the case if the temple building in front of the cave did not exist. If all doors in the present building were kept closed at all times, particle deposition onto horizontal surfaces within the cave would be reduced by about 81% relative to the hypothetical situation where the cave has no wooden structure in front of it and thus is completely open to the atmosphere, as is the actual case for the great majority of the caves at Yungang.

Next to examine is the passive filtration alternative in which filter material would be placed into the panels that exist around the surface of the shelter in front of Cave 6. Here are three subcases:

Subcase 1

All doors in the building would be kept closed but there would still be leakage of unfiltered outdoor air into the cave through cracks around the doors and/or window panels. Specially selected low-pressure drop filter material (type GSB-30, sold in China by Minnesota Mining and Manufacturing, Inc.) would be used to replace the paper that presently covers the windows in the wooden temple structure at the ground-floor and third-floor levels, leaving the appearance of the existing wooden building virtually unchanged. In Table 2, line 4, it is seen that this would not offer much

further improvement, with 17% of the mass of deposited particles relative to the base case still remaining. The reason for this is that, of the $34 \text{ m}^3 \text{ min}^{-1}$ of air that enters the cave, $24 \text{ m}^3 \text{ min}^{-1}$, or about 71%, of the flow into the cave would still pass unfiltered through the cracks in the building shell, and only the remaining 29% of the flow would pass through the filter material. The available filter cross-sectional area in this case is assumed to be equal to 2.56 m^2 each for both the downstairs and the upper levels of the wooden building front. This value is chosen because it is approximately equal to the cross-sectional area of the paper that exists behind the open latticework of the panels in the ground-floor level at the front of the present wooden temple structure.

Subcase 2

Filter material would be used to replace the paper windows in two floors of the existing building, as in the previous case, but particle deposition would be greatly reduced by caulking all cracks in the building shell, thus forcing all the air flowing into the cave (in this case about $6.3 \text{ m}^3 \text{ min}^{-1}$) to pass through the GSB-30 filters. As seen in line 5 of Table 2, the mass of particles deposited onto horizontal surfaces within the cave would then be only about 1% of the base case. Again, 2.56 m^2 of filter material is placed in both the upstairs and ground-floor surfaces of the existing temple front panels in this case.

Subcase 3

The very low airflow rate into and out of the cave in subcase 2 above could cause problems if air exchange rates affected the rate at which water vapor (arising from water seepage through the cave rock surface, which damages the sculptures) is exhausted from the caves. Therefore, an ability to move air in and out of the caves at volumes like those observed historically may be desired. This can be achieved by increasing the cross-sectional area available for placement of filter material in the surface of the building panels. This may be impractical at Cave 6 given the historical character of the present wooden temple building in front of that cave, but if new shelters were constructed for other caves that presently lack any shelters, then provision for placement of greater amounts of filter material in such new structures could be considered. Preliminary design studies performed by Sedlak (1991) suggest that modified shelters could be erected in front of the caves that currently do not have them, with a design that would allow for a surface area of 46 m^2 (at the ground level) and 55.4 m^2 (at the upper floors) for filter placement, in the face of a building the size of the one in front of Cave 6. Line 6 in Table 2 examines such a case, using a cave with the dimensions of Cave 6 and a shelter constructed without significant air leaks between panels, and with air locks at the entry doors to suppress infiltration of untreated air as doors are opened and closed. Using this greater exposed area of filter material, $86 \text{ m}^3 \text{ min}^{-1}$ of air would enter the cave. We see then that 97% of the particle mass flux can be suppressed relative to a cave with no shelter in front of it, and the time necessary to completely cover an upward-facing horizontal surface inside the cave with

the first monolayer of dust would be increased to 6.3 years under conditions like those observed on 15–16 April 1991. Actual soiling rates will be faster than this because annual average deposition fluxes are higher than during the 15–16 April events available for model calculations. Still, a 97% reduction in particle mass flux would be effected relative to annual average conditions at an unsheltered cave, which is a substantial improvement.

Conclusions

A number of control alternatives have been identified in Tables 1 and 2 that would result in a major reduction in the rate of deposition of coarse particles inside the Yungang grottoes. One method employs a standard mechanical ventilation system with either high-efficiency filters, or low-efficiency filters—like filter F_{A3} —that are loaded with collected particles (easily achieved at Yungang). This method could reduce deposition rates on horizontal surfaces to 3–4% of historically observed levels, provided that air leakage into buildings in front of the caves can be kept to no more than about 3% of the uncontrolled airflow through an unsheltered cave, or no more than about 10% of the historically observed airflow through a cave like Cave 6 that has an existing wooden shelter in front of it. The degree of control in this case is really determined by the air infiltration rate achieved. If air infiltration could be eliminated, then reduction to less than 1% of the historical deposition rate could be achieved, but we view complete elimination of infiltration as unlikely. The best performance that can be obtained from a passive filtration system is a reduction to about 3% of uncontrolled deposition rates for the case of a tightly constructed new shelter in front of a cave with approximately 100 m² of filter material incorporated into the outer surfaces of that building.

Choosing a control system for the grottoes is not an easy task. Although the 96–97% coarse particle deposition control efficiencies of fairly simple systems sound impressive, the outdoor air at Yungang is extremely dirty. As seen in the far-right column of Table 1 and of Table 2, the time required to produce 100% coverage of a horizontal surface at Cave 6 is less than one-half year at present. That first monolayer coverage by particles probably is sufficient to produce most of the objectionable visual character of the soiling problem. Beyond a full monolayer coverage by dust, the deposits simply get deeper. Indeed, much less than a full monolayer coverage by particles is noticeable to a human observer. A 0.2% coverage by dark particles on a white surface is detectable if one looks very closely (Hancock, Esmen, and Furber 1976), and a 1% coverage can be seen easily at close range. The exact point at which visitors viewing the statues from a distance would notice the soiling is not known, but it is surely less than the point at which 100% surface coverage is reached.

The time needed to accumulate the first full monolayer of deposited particles, either in the presence of several possible mechanical air-filtration systems with reduced (but not zero) air infiltration or in the presence of the most promising passive filtration system, is about six to eight years under 15–16 April 1991 conditions, and up to four times faster under annual average conditions (see lines 7, 8, 11, and 12 of Table 1 and

line 6 of Table 2). Noticeable soiling would occur in less time. Given the time and effort needed to clean and restore a cave once it gets dirty, such a high remaining particle flux may be unacceptable.

The alternative to accepting such rates for recurrence of 100% coverage of the horizontal areas of the statues would involve an all-out attack on the problem, including (1) careful attention to making any new buildings in front of the caves as airtight as possible, forcing nearly all air exchange through filters (air must still be exchanged with the outdoors through filters in order to exhaust water vapor that leaks through the rock walls of the caves, and stopping air exchange completely by sealing the caves could be disastrous); (2) selection of the best passive filtration system or mechanical filtration system that can be supported; and (3) suppression of the local outdoor dust sources, as described earlier.

One could also study the effect of control of local coal smoke and regional outdoor air pollution sources other than the local road dust and soil dust, if the State Bureau of Cultural Relics or the Yungang grottoes staff believe that such a control program would be possible.

In conclusion, several questions need to be resolved: At what point is an unacceptable level of soiling of the statues reached? Is it as little as the first point where a close observer would notice the soiling, or is it as much as a full monolayer of dust or more? For how long must the statues remain cleaner than this unacceptable level of soiling?

Once these questions have been answered, the methods developed during the present analysis can be used to support the selection of an actual control system.

Acknowledgments

This work was supported by a research agreement from the Getty Conservation Institute. The cooperation and assistance of the staff of the Yungang grottoes and the State Bureau of Cultural Relics are gratefully acknowledged, including Huang Kezhong, Zhu Changling, Sheng Weiwei, Li Xiu Qing, Li Hua Yuan, Xie Ting Fan, Yuan Jin Hu, Huang Ji Zhong, and Zhi Xia Bing. The authors also extend their thanks to Bo Guo Liang of the Shanxi Institute of Geological Sciences, and Zhong Ying Ying from Taiyuan University. Assistance critical to this work was provided by the Getty Conservation Institute and its consultants, and we especially thank Neville Agnew, Po-Ming Lin, Shin Maekawa, and Roland Tseng for their help.

References

- Christoforou, C. S., L. G. Salmon, and G. R. Cass
1994 Deposition of atmospheric particles within the Buddhist cave temples at Yungang, China. *Atmospheric Environment* 28:2081–91.
- Hancock, R. P., N. A. Esmen, and C. P. Furber
1976 Visual response to dustiness. *Journal of the Air Pollution Control Association* 26:54–57.
- Nazaroff, W. W., and G. R. Cass
1989 Mathematical modeling of indoor aerosol dynamics. *Environmental Science and Technology* 23:157–66.

- Nazaroff, W. W., M. P. Ligocki, L. G. Salmon, G. R. Cass, T. Fall, M. C. Jones, H. I. H. Liu, and T. Ma
1993 *Airborne Particles in Museums*. Research in Conservation series. Marina del Rey, Calif: Getty Conservation Institute.
- Nazaroff, W. W., L. G. Salmon, and G. R. Cass
1990 Concentration and fate of airborne particles in museums. *Environmental Science and Technology* 24:66–77.
- Salmon, L. G., C. S. Christoforou, and G. R. Cass
1994 Airborne pollutants in the Buddhist cave temples at the Yungang grottoes, China. *Environmental Science and Technology* 28:805–11.
- Salmon, L. G., C. S. Christoforou, T. J. Gerk, G. R. Cass, G. S. Casuccio, G. A. Cooke, M. Leger, and I. Olmez
1995 Source contributions to airborne particle deposition at the Yungang grottoes, China. *Science of the Total Environment* 167:33–47.
- Sedlak, V.
1991 *Report on a Conceptual Design for a Protective Portico/Facade for Cave 19, Yungang Grottoes, Shanxi Province, PRC*. Randwick, Australia: Vinzenz Sedlak Proprietary Limited.

Microclimate of Cave Temples

53 and 194, Mogao Grottoes

Sadatoshi Miura, Tadateru Nishiura, Zhang Yongjun, Wang Baoyi, and Li Shi

SINCE 1986, the Tokyo National Research Institute of Cultural Properties and the Dunhuang Academy have worked together for the conservation of the Mogao grottoes at Dunhuang. An agreement for this joint project was signed in December 1990 and includes three types of research on the grottoes: an environmental study, an analysis of deterioration, and a conservation study. The following is based on the environmental study of two grottoes from 1988 to 1992.

The Mogao grottoes consist of 492 cave temples excavated in a cliff above the Daquan River. The caves are situated at three levels—upper, middle, and lower—and vary considerably in dimension. While some can accommodate only one person at a time, others are large enough for many visitors.

The hypothesis was that different kinds of deterioration are caused by the different climatic conditions that may exist in certain caves. Caves 194 and 53 were chosen for measurement (Fig. 1). As Cave 194 is located on the upper level of the cliff and Cave 53 is on the lower level, the two caves were assumed to have different microenvironments, which would lead to different kinds of damage to their wall paintings (Miura et al. 1990).

Cave 194 is rather small. Its dimensions are approximately 3.6×3.6 m in depth and width, with a height of 3.3 m. The grotto has an antechamber and a lateral grotto, known as Cave 195. The paintings in Cave 194 are mainly from the Tang dynasty and are still intact today. Many small areas of flaking are found by careful observation, however, as well as blistering of the paint surface.

Cave 53 is large, with dimensions of about $6.5 \times 6.5 \times 6.5$ m. It also has a lateral grotto, Cave 469, the entrance of which was sealed during the measurement period. Sand to a depth of several meters had covered the floor of Cave 53 until the 1960s. In the past, river water had often entered through the front of the cave, giving rise to humid conditions that caused flaking of the paint and black spots on the lower part of the wall.

Measurements

The microclimates of the two grottoes have been measured since March 1988 to investigate the causes of deterioration. Figure 1 shows the location

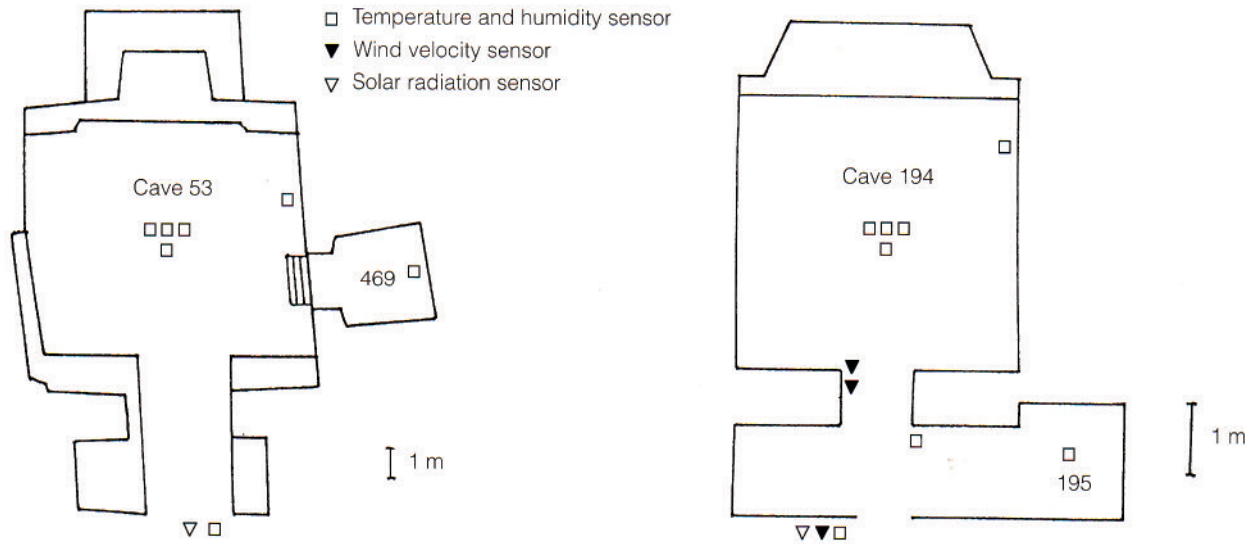


Figure 1
 Plan of Caves 53 and 194.

of sensors. Temperature and humidity have been measured at three different heights at the center of each grotto. Since May 1991, temperature and humidity have also been measured inside a hole drilled in the ceiling of Cave 194 and in the floor of Cave 53.

Climatic data were recorded in data loggers every two hours (twelve times a day) from March 1988 to May 1991 (Li et al. 1990), and every hour (twenty-four times a day) from May 1991. The data are collected by a portable computer at the grotto or at the laboratory of the Dunhuang Academy by a radio system.

Average, maximum, and minimum climatic values are calculated from daily data. Monthly and annual values are derived from these daily calculations. Since Cave 194 is heated by sunlight during the day, the temperature measured at the entrance of this cave does not represent a typical outside value. Temperature and humidity measurements at the entrance of Cave 53 are used, therefore, as the external values for both grottoes.

Internal-external differences

Annual temperature changes within the grottoes were found to be less than the changes in temperature outside (Miura et al. 1992). Daily temperature and humidity changes in both grottoes were also less than those of outside. Only the annual humidity change did not show this tendency.

Even though Cave 469 is sealed from the outside, its humidity varies more than that of Cave 53 (Miura et al. 1992). This fact suggests that heat from outside is isolated by the rock but that moisture from outside (rain or groundwater) still affects the inside humidity via the rock.

Vertical differences inside the grottoes

The grottoes have an internal vertical temperature difference of about 4–5 °C from floor to ceiling on monthly average. It is interesting that the daily amplitudes of temperature at ceiling and floor depend on the season. Daily temperature at the ceiling changes more in summer (2.6 °C in July)

and less in winter ($0.3\text{ }^{\circ}\text{C}$ in January), whereas daily temperature at the floor varies in reverse ($0.3\text{ }^{\circ}\text{C}$ in July and $2.7\text{ }^{\circ}\text{C}$ in January). This indicates that warm outside air enters a grotto along the ceiling in summer, and cold outside air enters over the floor in winter. A slow airflow was actually observed at the floor of a corridor of Cave 194 in winter. Air also circulates inside the grottoes, and its direction of flow changes according to the season.

Differences between grottoes at different levels

The average temperature of Cave 194 is higher (about $2\text{ }^{\circ}\text{C}$) than that of Cave 53 (Fig. 2). Evidently the rock layer above Cave 194 is not thick enough to insulate the grotto from the heat of the sun.

One hole was drilled in the ceiling of Cave 194 and another in the floor of Cave 53 to study the microclimate in detail. Results show that humidity in both holes is high throughout the year (Fig. 3). Although the temperature in the hole of Cave 53 was more stable than that measured in the grotto itself, the temperature in the hole of Cave 194 was higher than that measured elsewhere in this grotto, which demonstrates the heating effect of sunlight on this cave.

The absolute humidity (moisture content in air) measured in the two holes was always higher than that of the outside air (Fig. 4), which indicates that the rock is more humid than the air. In particular, the hole in the ceiling of Cave 194 is much more humid than the hole in the floor of Cave 53. This would be very strange if the moisture had come from the river, because Cave 194 is located about 20 m higher than Cave 53 and

Figure 2
Climatograph of Caves 194 and 53: ● indicates outside data, ○ represents the inside of Cave 194, and ○ represents the inside of Cave 53.

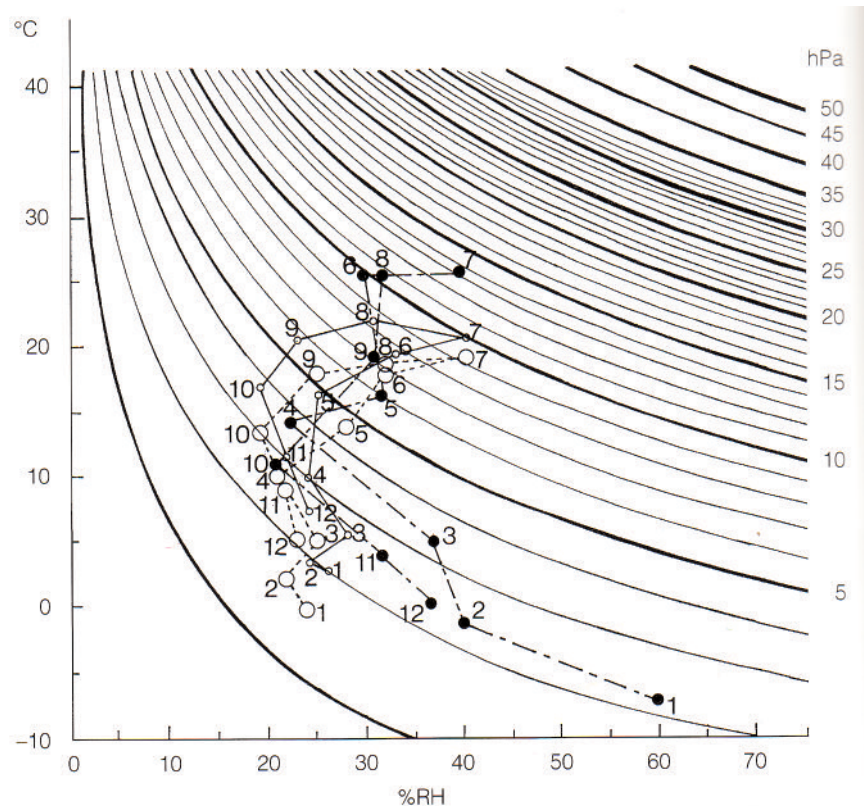


Figure 3
 Temperature and humidity measurements taken in the holes in the ceiling of Cave 194 and the floor of Cave 53.

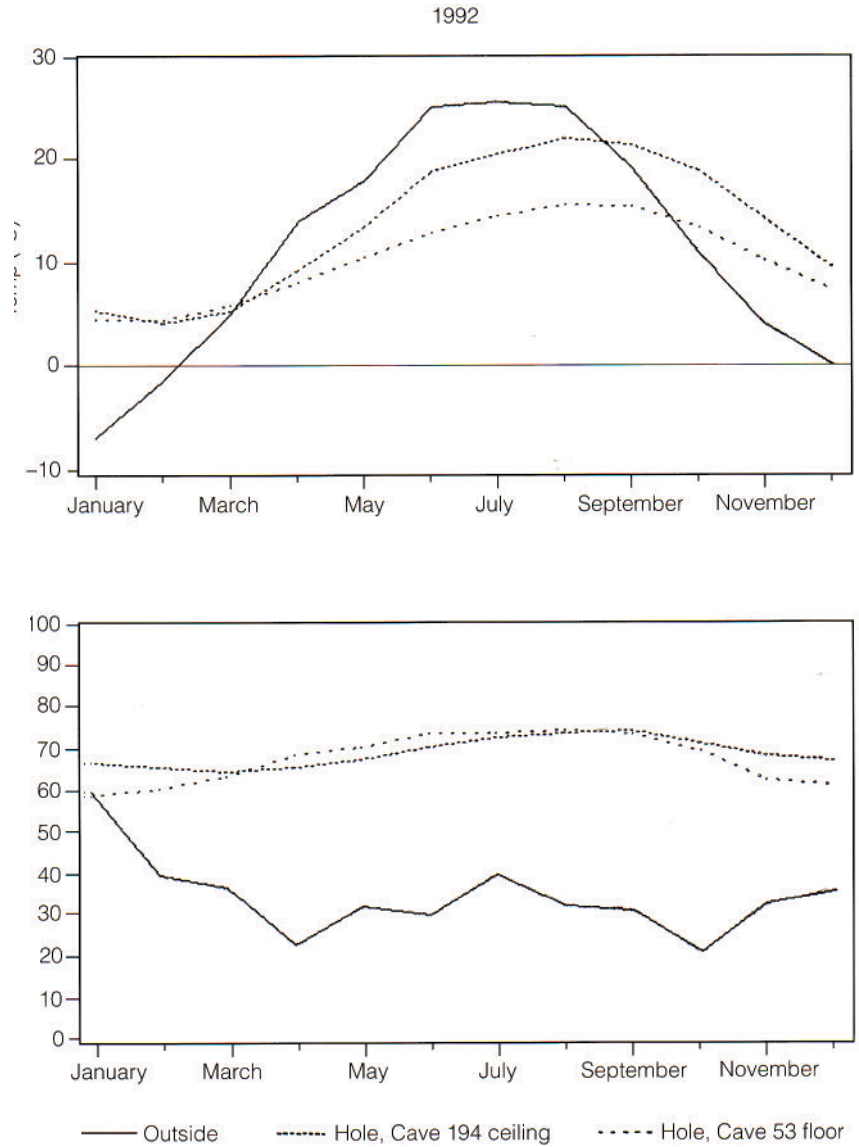
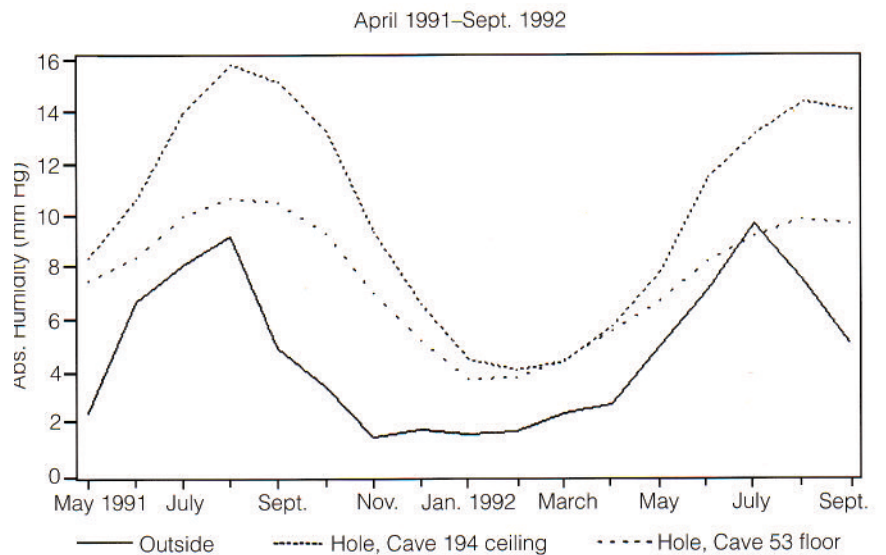


Figure 4
 Absolute humidity measurements taken in the holes.



30 m above the river. An explanation may be found in Figure 5, which shows that the seasonal change in absolute humidity corresponds to the amount of rainfall.

The following conclusion was made: Rain soaks into the ground above the cliff and collects on the rock roof above Cave 194, since it is located below a small depression. The permeating rainwater carries soluble salts, which are found in high concentration in the surrounding sand and rock, into the grotto. The soluble salt, halite (NaCl), effloresces on the surface of the wall paintings when the water evaporates (Kuchitsu and Duan 1992), and damage to the paintings, such as blistering and flaking in spots, takes place. Since rainwater comes from the top of the cliff, the damage is more severe on paintings near the ceiling.

One early restoration attempt caused unexpected damage to the paintings. Decades ago, some of the areas affected by flaking were treated with a white mortar. After this intervention, damage by rainwater increased because water could not penetrate the mortar. More water evaporated from the surface of the paintings, and more efflorescence resulted.

Between 1961 and 1980, Dunhuang experienced heavy rain and flooding once. From a statistical analysis of climatic data during that period, a maximum rainfall of more than 20 mm day⁻¹ probably occurs about once every fifteen years in Dunhuang (Fig. 6) (Takahashi et al. 1994). Such heavy rainfall can cause major damage, and it is important to protect cave paintings from these occasional events.

Conclusions

This study shows the influence of rainfall and groundwater on the microclimate of the grottoes. The following conclusion is derived from the two caves studied: Cave 194, located at the upper cliff level, suffers damage from efflorescence of halite as a result of moisture infiltration from above and migration through the rock. Cave 53, located at the lower level, shows efflorescence of a different salt: gypsum (Kuchitsu and Duan 1993),

Figure 5
Rainfall data at Mogao grottoes from April 1991 to September 1992.

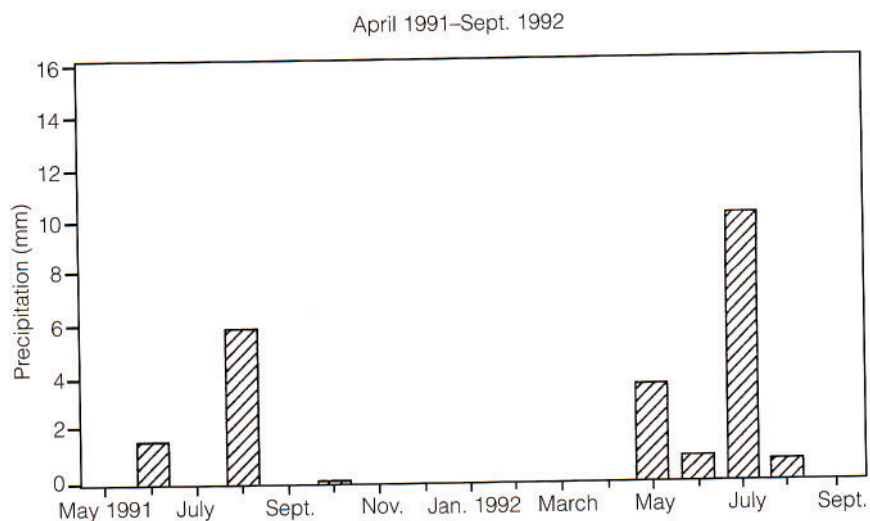
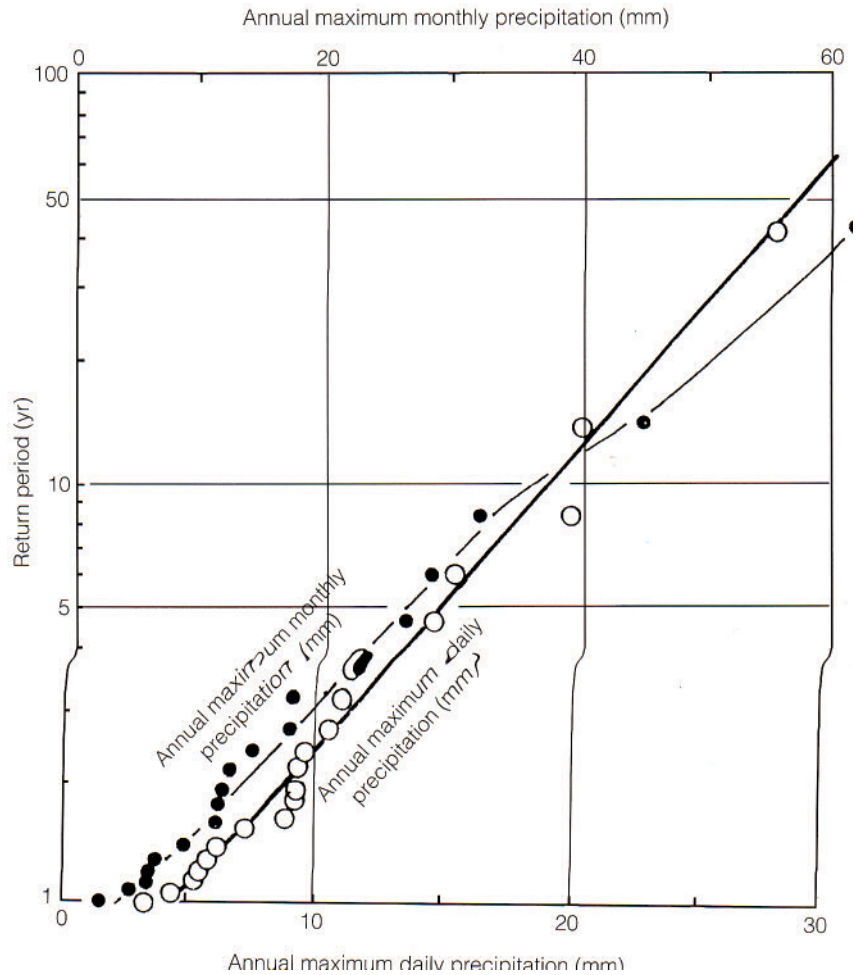


Figure 6
Return period of annual maximum monthly
and annual maximum daily precipitation.



which may be produced by reaction between river water and soil when flooding occurs.

Thus, the wall paintings in these grottoes deteriorated mainly because of water, even though Mogao is located in a desert region. Rainwater moves through the rock of a grotto, then evaporates from the surface. Seasonal air circulation in the grottoes probably accelerates evaporation. This process causes flaking of the wall paintings in spots by efflorescence of soluble salts.

Protection from rainwater is important, especially for Cave 194. Installing a drainage system at the top of the cliff may be one effective means of conservation. Inadequate measures that may accelerate deterioration should be avoided.

Acknowledgments

This joint work has been carried out with the help of many colleagues in China and Japan. The authors would like to express their sincere thanks to them, especially to the staffs of the State Bureau of Cultural Relics in Beijing, the Agency of Cultural Property of Gansu Province, the Dunhuang Academy, the Agency of Cultural Affairs in Japan, and Tokyo National Research Institute of Cultural Properties.

References

- Kuchitsu, Nobuaki, and Duan Xiuye
1992 Geological environment of the Dunhuang Mogao grottoes, Gansu Province, China. *Hozon Kagaku* 31:79–85.
- 1993 Salt crystallization and deterioration of mural paintings in the Dunhuang Mogao grottoes, Gansu Province, China (in Japanese). *Hozon Kagaku* 32:28–34.
- Li Shi, Zhang Yongjun, Sadatoshi Miura, and Tadateru Nishiura
1990 Meteorological observations at Dunhuang, Mogao (in Chinese). *Dunhuang Yanjiu* 1:108–14.
- Miura, Sadatoshi, Tadateru Nishiura, Li Shi, and Zhang Yongjun
1990 Climate in the Mogao grottoes (in Japanese). *Hozon Kagaku* 29:1–7.
- 1992 Climate at Dunhuang Mogao grottoes from 1989 to 1991 (in Japanese). *Hozon Kagaku* 31: 87–94.
- Takahashi, Hidenori, Sozo Fujita, Sadatoshi Miura, Zhang Yongjun, and Wang Baoyi
1994 Climate at Dunhuang Mogao grottoes (3): Characteristics of heavy precipitation in Dunhuang (in Japanese). *Hozon Kagaku* 33:27–34.

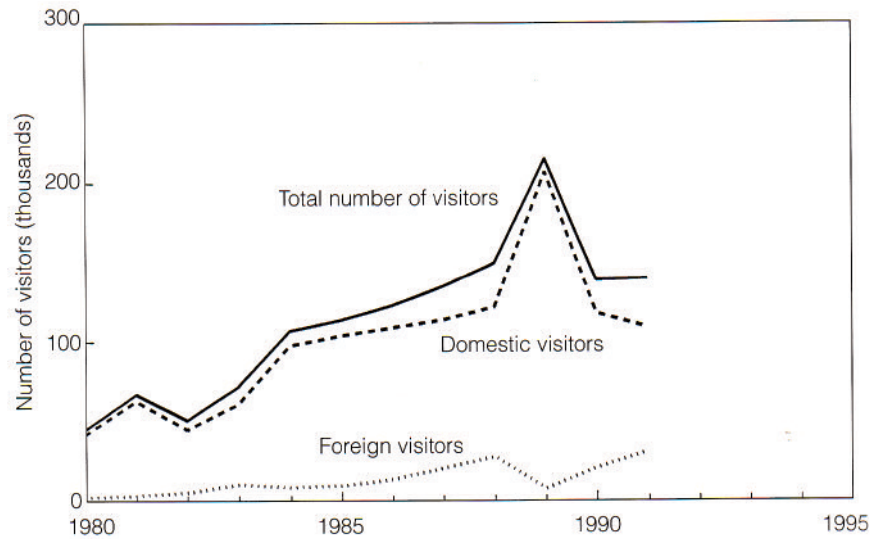
Environmental Monitoring at the Mogao Grottoes

Shin Maekawa, Zhang Yongjun, Wang Baoyi, Fu Wenli, and Xue Ping

THE MOGAO GROTTOS are located approximately 25 km southwest of the city of Dunhuang in Gansu Province in Northwest China, between the Gobi and Takla Makan deserts. Situated along the ancient Silk Road, it maintains one of the world's richest collections of Buddhist murals and statues dating back from the fourth to thirteenth century C.E. The caves were excavated in various sizes and shapes into a natural cliff approximately 30–50 m high, running roughly north-south. The rock consists of a soft, poorly cemented, coarse conglomerate. In the 492 decorated grottoes, mud plaster mixed with straw was laid directly on the conglomerate surface, and a white ground-paint layer was applied prior to the application of the succeeding paint layers.

Over the centuries, the priceless Buddhist artifacts, wall paintings, and clay sculptures in the grottoes were constantly subjected to looting or deliberate defacement. The Dunhuang Academy was established at the site in 1944 to protect the sites and conduct research on the history and culture of the Dunhuang region. The recent economic boom, political change, and widespread cultural awareness of the Asian region have facilitated a sharp increase in the number of tourists visiting the site (Fig. 1). The large number of visitors could change the microclimate of the caves, which can be deleterious to the murals and statues; continued high relative humidity levels produced by visitors may allow growth of fungi and bacteria, which could lead to permanent staining of the wall paintings (ASHRAE 1993; Torraca 1984:1–18). On the other hand, an extremely dry microenvironment in the caves resulting from the intrusion of dry desert air may desiccate the paint layers, resulting in flaking of the painted surfaces (Maekawa 1993:616–23). Fatigue failure of the paint layers may result if the wall paintings are subjected to large daily variations of temperature and relative humidity. Large numbers of visitors could also produce a high enough concentration of carbon dioxide in the caves to be unsafe for the visitors themselves (ASHRAE 1993). Furthermore, the combination of the high relative humidity and carbon dioxide could result in formation of carbonic acid, which could alter the painting surface.

Figure 1
Number of domestic and foreign visitors at
the Mogao grottoes between 1980 and 1991.



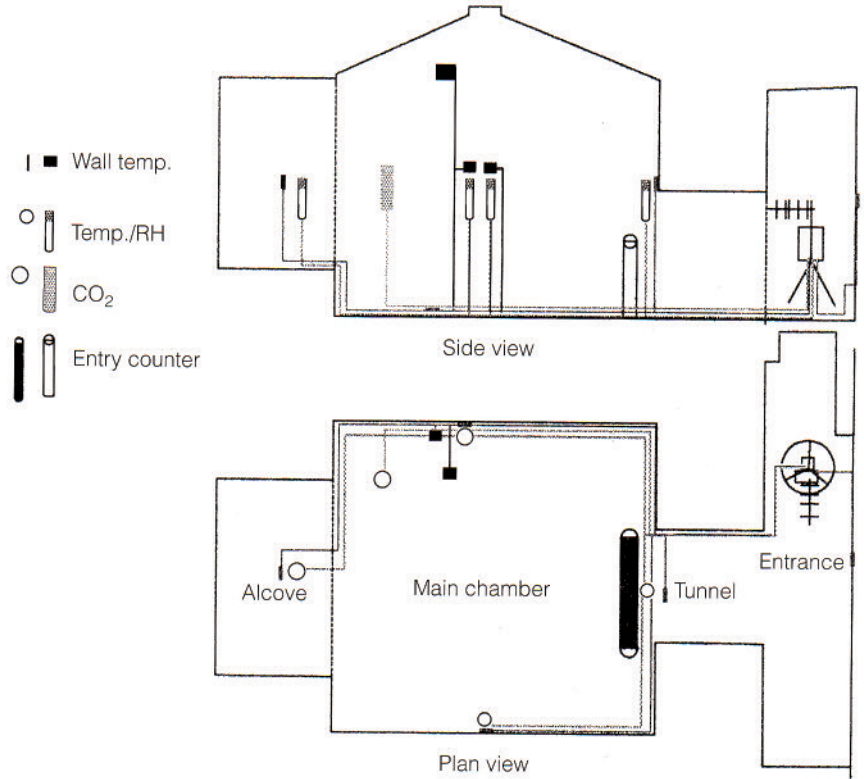
Objectives

Before any conservation work on a monument can be planned, basic information on the natural and fabricated environments affecting the site is needed. In the case of the grottoes, a dry desert climate combined with the stable microenvironment of caves contributed to the survival of the wall paintings and sculptures. However, the constant increase of visitors may be altering the microenvironment. Thus, in addition to general information on the climate of the site and microclimate of the caves, information was gathered about the effects of visitation on the caves' microenvironment: changes in cave temperature, relative humidity (RH), and carbon dioxide content. The number of visitors and their length of stay in the caves, as well as the months of maximum cave visitation, were also important factors to be documented. The ultimate objective of the environmental monitoring was to develop strategies to reduce the effects of visitors on the microenvironment of the grottoes.

Model Caves

Two architecturally similar, medium-size caves, Caves 323 and 335 (Fig. 2), were selected to document effects of visitors on the microenvironment. Both are located at ground level (there are no caves below them), oriented east to west. As indicated in Figure 2, each cave consists of a main chamber of about 125 m³ with an alcove of approximately 25 m³ and an entrance area of approximately 24 m³, connected by a short tunnel approximately 2 m high, 1 m wide, and 2 m long. Each cave has been fitted with a wall made of aluminum sheets on which two hinged doors, approximately 1 m wide and 1.8 m high each, are mounted in the middle. Both the wall and doors are made with fixed-angle louver openings. In 1989, as part of the collaborative conservation project of the Getty Conservation Institute and the Dunhuang Academy, a filter material was installed over the openings of the caves to protect against the intrusion of airborne sand and dust. The material used was a nonwoven, spun-bound, lightweight

Figure 2
Schematic of Caves 323 and 335.

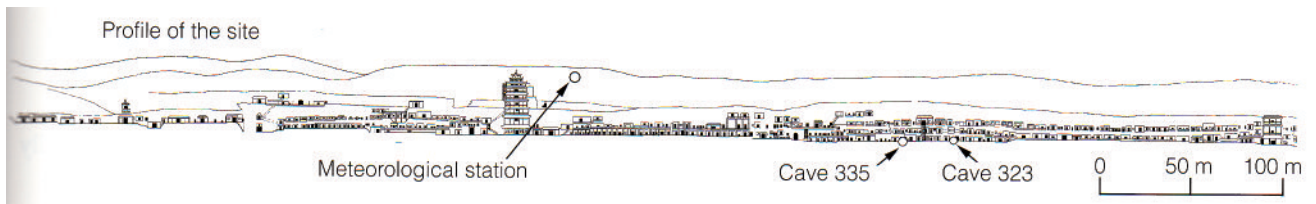


geotextile. Thus, it was expected that air exchange rates would be significantly reduced. Cave 323 was normally open to visitors for eight hours each day, and thus became the test cave. Cave 335 was closed to visitors, and served as the control.

Monitoring System

Three autonomous, environmental monitoring stations (one meteorological and two cave stations) and a base receiving station were installed (Figure 3 shows their locations). The meteorological station for collecting area-wide climatic data was located on top of the 35 m high cliff near the center of the site and approximately 200 m from the base station, which was set up at the Dunhuang Academy's laboratory building on the site. Cave stations were configured to gather information within the environment of the individual caves, which are approximately 250 m north of the meteorological station. The retrieval procedure for the accumulated environmental and microenvironmental data consisted of periodically transmitting the data collected at each station via UHF radio to the base station, where they were transferred to microdiskettes. These diskettes were then mailed to the Getty Conservation Institute in California for statistical analysis.

Figure 3
Map of the Mogao grottoes and locations of monitoring and base stations.



Continuous monitoring

Visitor groups seemed to spend about five minutes in Cave 323, since it is of medium size. Therefore, a two-minute interval was chosen to monitor environmental changes in Cave 323 and yielded at least two measurements during visitation periods. At night, when there were no visitors, the interval was extended to fifteen minutes to improve the efficiency of the data collection and maximize the equipment's capacity. Four sets of air-temperature, RH, and surface-temperature sensors were placed between the entrance and the alcove, at the deepest location in the main chamber of the cave. The air-temperature and RH sensors were mounted on self-standing glass panels (installed by the Dunhuang Academy to protect the paintings from being touched), positioned 20–30 cm from the walls. Each surface-temperature sensor was first adhered to an oversized strip of thin cotton gauze, then the perimeter of the strip was mounted on the painted surface using Paraloid B-72 adhesive diluted with acetone to ensure reversibility. An additional set of wall-temperature sensors was located 2 m from the floor and near the ceiling to determine any variation in wall temperature with respect to height. A set of infrared-photo sensors was placed at the entrance of the main chamber to log visitor entry and exit. Finally, a carbon dioxide monitor was positioned at the back of the main chamber. The same configuration of sensors, with the exception of the CO₂ sensor, which was omitted, was used in the control grotto.

Controlled experiments

The effects of visitor groups on the microenvironment of the caves were recorded through a number of controlled experiments conducted with the participation of visitors to the site. A group consisting of twenty to forty persons entered the main chamber of Cave 323 and stayed for thirty minutes while the entry doors were fully open. The group remained standing for the duration of the stay, then promptly exited. The entry door was closed immediately after exit. Three separate experiments were conducted to determine increases in the environmental parameters during the experiment and their subsequent decay.

Results of Environmental Monitoring

Climate of the site

The climate of the Mogao region is arid, with seasonal extremes of temperature. At the top of the cliff, the air temperature varies from -15°C in February to 38°C in July, with the daily minimum relative humidity ranging from 28% in February to only 10% in July. Throughout the day, the RH typically remains between 10% and 20% in summer months and 20% and 30% in winter months, except for the occasional passing of a moist air mass through the area, associated with movements of weather fronts in the region. The typical diurnal temperature variation is approximately 15°C throughout the year. During the testing period, medium strength wind, averaging 5 m s^{-1} , was always present. The wind direction normally

shifted to the south and southeast during the day, and to the southwest at night. Gusty westerly winds generated dust storms in spring. The daily maximum solar radiation ranged between 1.0 kW m^{-2} in June and 0.4 kW m^{-2} in December. Rainfall was concentrated in the summer months of June, July, and August, with an annual total rainfall of about 25 mm. Snow was observed in the winter months, but accumulation was not recorded.

The microclimate of the site below the desert plateau, directly outside Cave 335 at the base of the cliff, was milder: $-10 \text{ }^\circ\text{C}$ in February, $30 \text{ }^\circ\text{C}$ in July, and 17% RH in April versus 35% RH in August. The monthly average moisture content of the air (expressed in the humidity ratio, which is the weight of moisture in one kilogram of air at that temperature) ranged between 1.2 g of moisture per kg of dry air in January to 6.3 g of moisture per kg of dry air in August.

Microclimate of the control cave

Inside Cave 335, temperatures were more stable than outside, and the air temperature was higher (between $5 \text{ }^\circ\text{C}$ in February and $19 \text{ }^\circ\text{C}$ in August) while the low RH was 19% in January compared with a high of 42% in August. Air temperature was extremely stable throughout the day. Although the relative humidity was also relatively stable throughout the day, it varied day to day as it followed changes of the outside climate, particularly during summer. The average monthly humidity ratio of the air in the cave varied between 5.5 g of moisture per kg of dry air in August and 1.2 g of moisture per kg of dry air in February.

Surface temperatures of the cave walls remained only $1\text{--}2 \text{ }^\circ\text{C}$ higher in winter and $1\text{--}2 \text{ }^\circ\text{C}$ lower during summer than the temperature of the adjacent air. Therefore, the relative humidity of the wall surface, which was estimated from the moisture content of the adjacent air and the surface temperature of the wall, remained within 5% of that of the air. Temperature variations between floor and ceiling remained less than $1 \text{ }^\circ\text{C}$; temperatures at the ceiling were higher than temperatures at the floor at all times. As expected, the influence of outside air was always greater near the entrance.

Microenvironment of the test cave

Visitors

Over 80% of the annual visitation total of forty-three thousand to Cave 323 was concentrated in the tourist season, between May and October, with the maximum number of visitors (thirteen thousand) in August. The number dropped to less than two thousand by October, and there were only small numbers of visitors in winter months, November through March. Figure 4 shows that in August there were occasionally up to eight hundred visitors per day. Figure 5 shows the distribution of visitors in an eight-hour day of operation during the busiest month, August. Admission to the cave is allowed between 8 A.M. and noon and between 2 and 5 P.M. On a daily basis, a large number of visitors visited the cave at about 9 A.M. and again at about 3 P.M. There were more visitors in the morning than

Figure 4
Daily total number of visitors to Cave 323 in 1991.

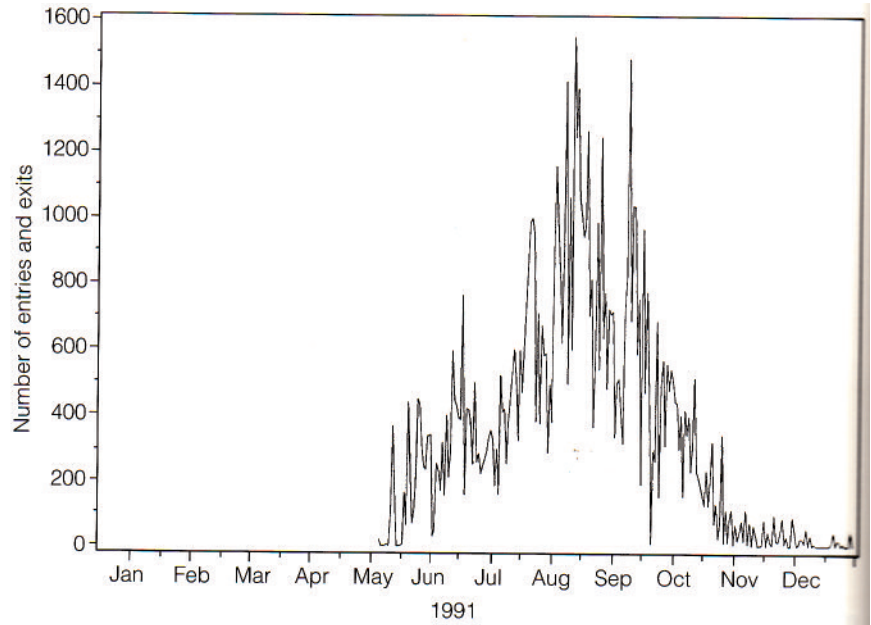
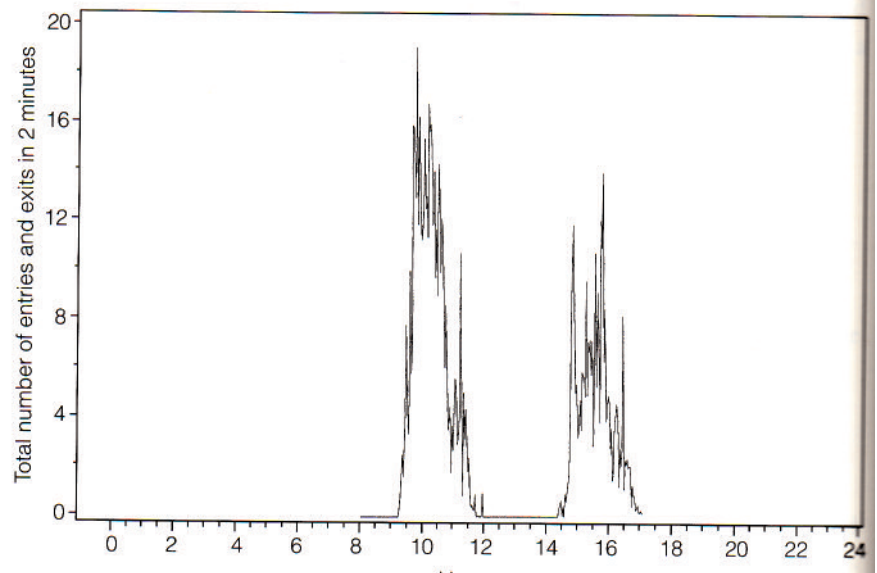


Figure 5
Daily distribution of visitors to Cave 323 in August 1991.



the afternoon, with an average of about six people per two-minute period around 10 A.M., while around 3 P.M. there were about two people per two minutes. The typical visit lasted about five minutes.

Air temperature

Figure 6 shows the daily extremes of air temperature in the cave. The smooth line connecting minimum temperatures indicates the natural air temperature change in the cave. The maximum temperatures exhibited extreme variations, particularly in the summer months when the greatest number of visitors tour the site, producing large daily variations in air temperature. Visitors always cause sharp increases in air temperature. Figure 7 shows the changes of air temperature between 8 A.M. and 5 P.M.

Figure 6
Daily extremes and average of air temperature in Cave 323 in 1991.

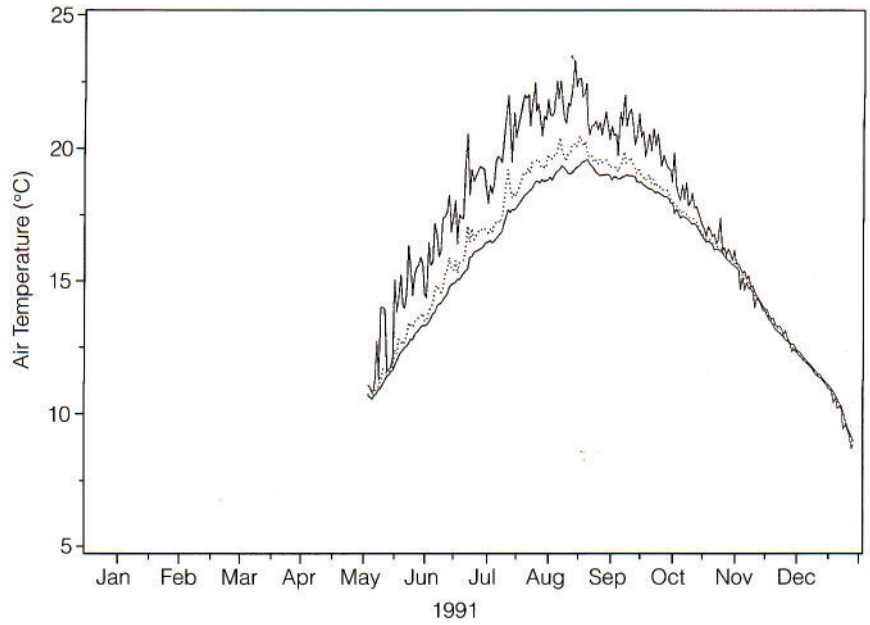
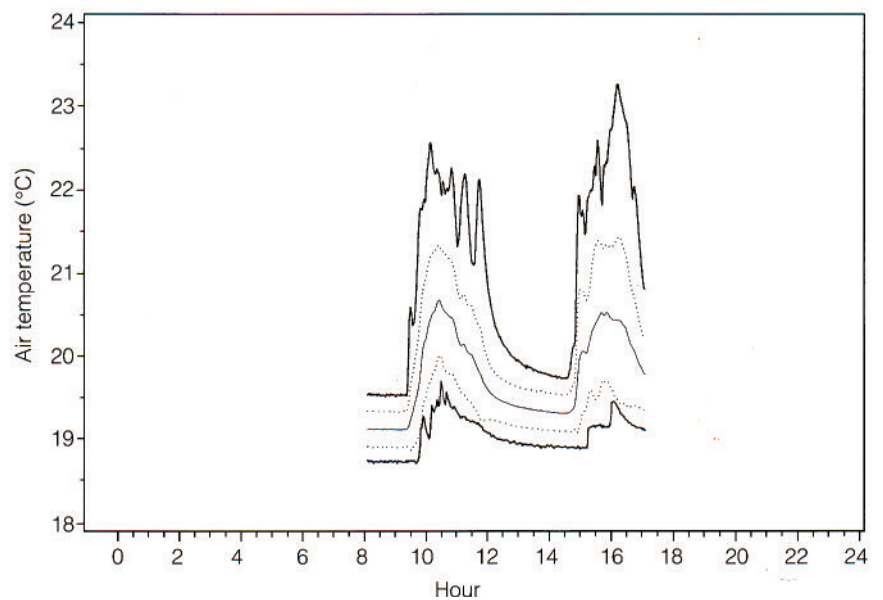


Figure 7
Daily changes of air temperature in Cave 323 in August 1991.



recorded in the visited cave in August 1991. Two peaks were recorded daily, and larger peaks were often recorded in the afternoon, although more visitors were logged in the mornings, indicating the strong effect of warmer, outside air. By the next morning in summer months, the temperature recovered to its natural level. Outside air temperature was always higher than the temperature in the cave during visitation hours. This resulted in increased air temperature in the cave whenever the entry door was opened.

Relative humidity

Daily extremes and averages of relative humidity in Cave 323 are shown in Figure 8. Unlike the relatively stable minimum air temperature in the cave,

Figure 8
Daily extremes and averages of relative humidity in Cave 323 in 1991.

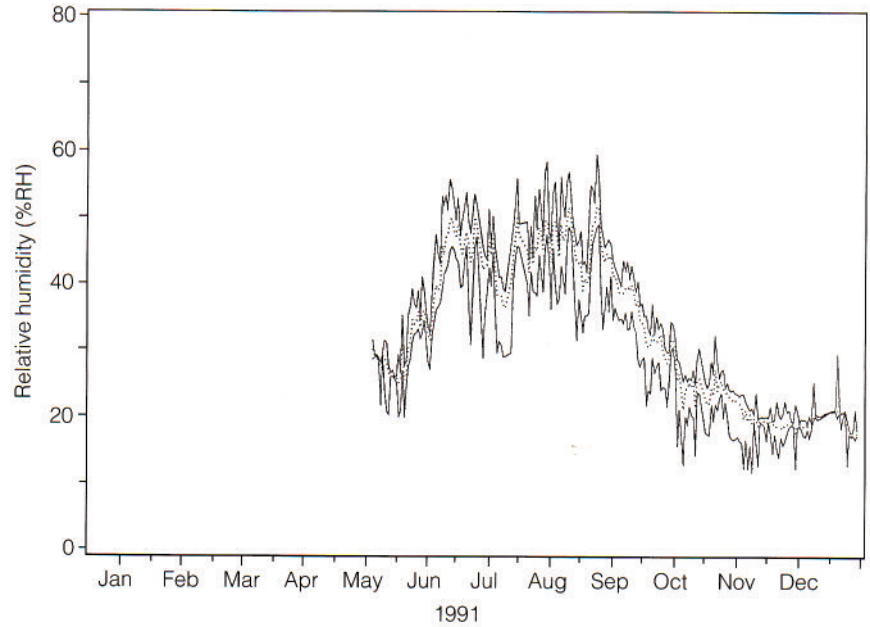
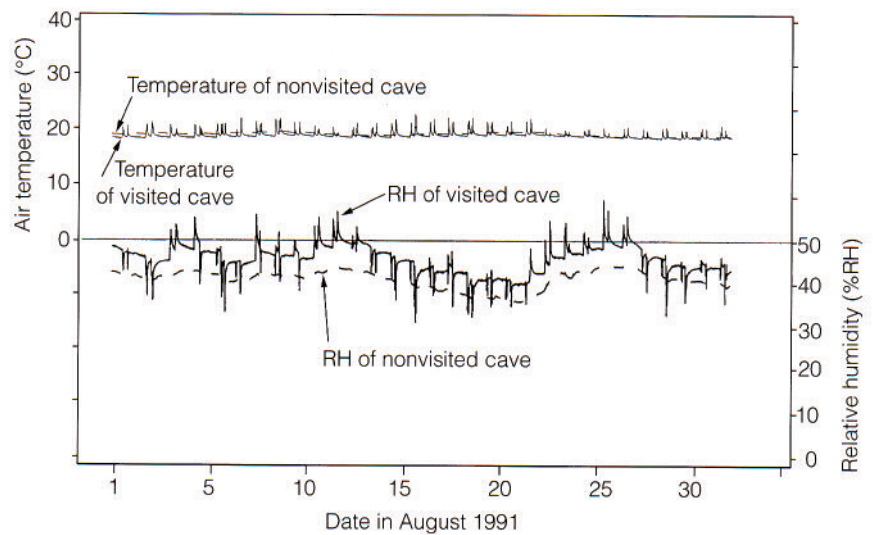


Figure 9
Air temperature and relative humidity changes in Caves 323 and 335 in August 1991.

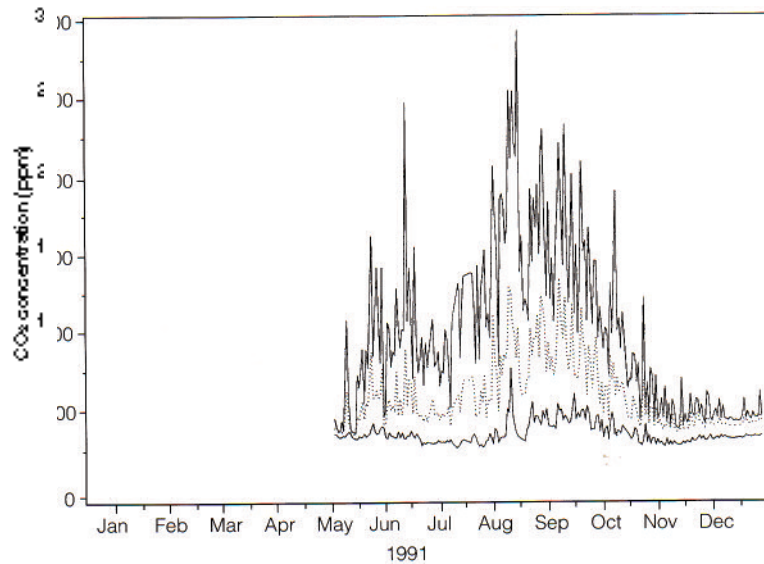


large daily variations of both the maxima and minima were recorded. This indicates that the effect of visitors is not limited to the increased relative humidity, which was expected as a result of visitors emitting moisture in the cave. Figure 9 shows comparisons of temperature and relative humidities in the test and control caves in August 1991. The baseline relative humidity of the visited cave was approximately 5% higher than that of the nonvisited cave, although changes in the moisture content of the outside air were also tracked. Twice-daily spikes, $\pm 3\%$ to $\pm 15\%$ RH, correlated precisely with the morning and afternoon surges of August visitors.

In spite of the expectation that spikes in the relative humidity in the visited cave would always be positive, as respiration leaves moisture in the cave, the spikes were both positive and negative relative to the stable

Figure 10

Daily extremes and averages of carbon dioxide levels in Cave 323 in 1991.



value, as seen in Figure 9. Negative spikes were always observed when the relative humidity in the cave was dropping for periods longer than a day; positive spikes were observed whenever the relative humidity was rising, which was due to changes of the moisture content of the outside air. The degree of influence of the outside climate on the microenvironment of the cave increased as the number of entries increased. The cause of these changes is due not only to the moisture released by the visitors, but also to the frequent opening and closing of the cave door and entry of visitors, which forced air exchange with the outside air.

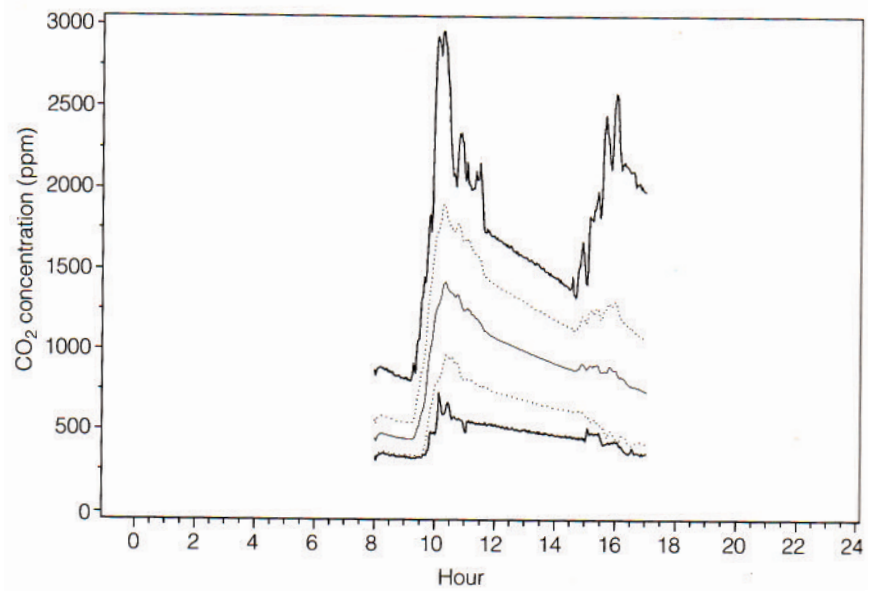
Temperature of the wall surface

Temperature differences between the wall surface and the air adjacent to it were quickly lost when visitors entered the cave, causing air turbulence. The result is a loss of the wall's protective thermal boundary layers, which causes the wall temperature to become equivalent with the air temperature. This phenomenon eliminates the possibility of condensation on the wall surface even on a rainy day. Therefore, temperature difference was not considered important in this study.

Level of carbon dioxide

Daily extremes and averages of carbon dioxide in Cave 323 in 1991 are plotted in Figure 10. The maximum concentration of carbon dioxide, approximately 3,000 ppm, was recorded in August 1991. The concentration always dropped to less than 700 ppm by morning, even when daily maximums reached more than 2,000 ppm. As expected, increase in the carbon dioxide content of cave air correlated well with the distribution of visitors, rising from a normal level of about 400 ppm to an average of some 1,500 ppm in the morning (and a maximum of nearly 3,000 ppm) when the cave received the most visitors (Fig. 11). From these high values, carbon dioxide concentrations dropped to an average of 1,000 ppm in the late afternoon and then recovered to the 500 ppm level by the next morning.

Figure 11
Daily changes of carbon dioxide levels in Cave
323 in August 1991.



Dust

The filter material mounted on the door openings was effective in eliminating the intrusion of windblown sand. However, the amount of airborne dust was insignificant in comparison to the amount of sand that was transported into the cave by visitors' shoes and clothes. A large volume of coarse, sandy dust, 0.1–0.5 mm in diameter, was found in the entryway to Cave 323.

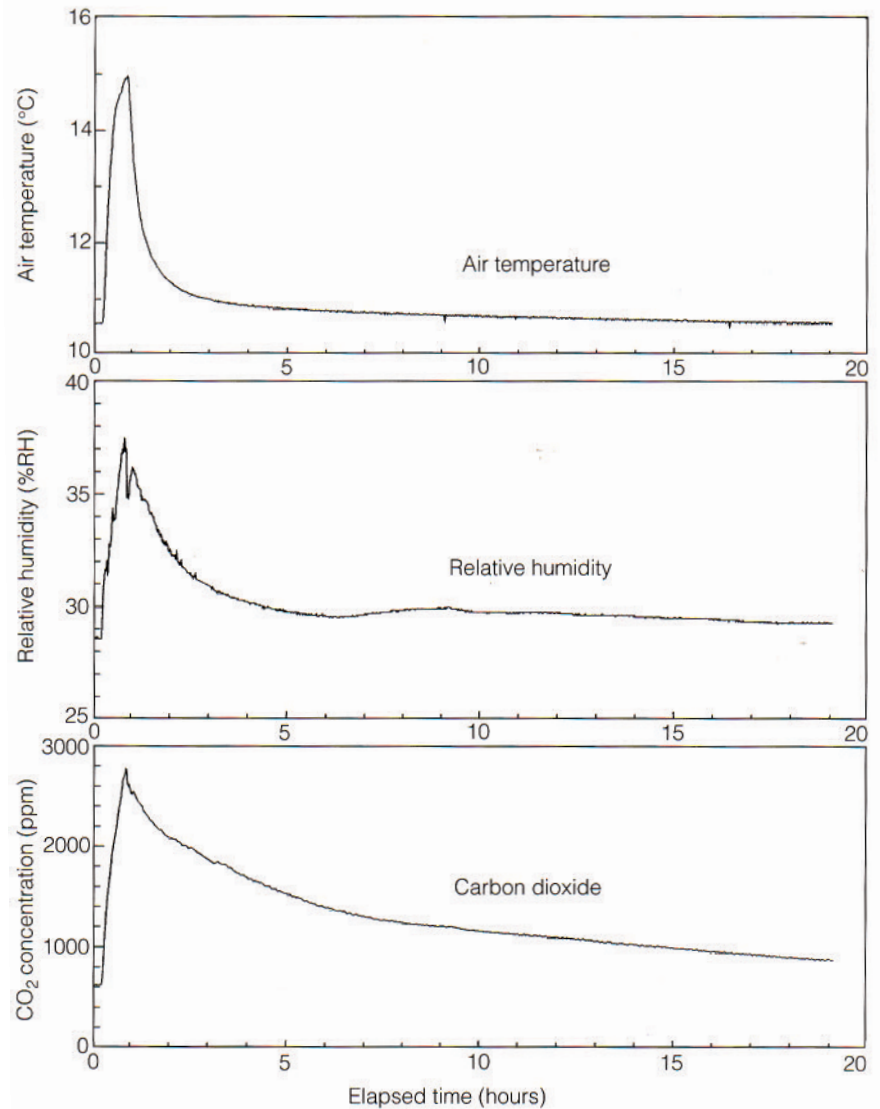
Results of Controlled Experiments

Figure 12 shows monitored changes of the air temperature, relative humidity, and carbon dioxide during one of the controlled experiments conducted in Cave 323. Averages of the measured rate of increase of environmental parameters during the controlled experiments were approximately 90 ppm per hour per person, 0.3% RH per hour per person, and 0.3 °C per hour per person, for carbon dioxide, relative humidity, and air temperature, respectively. The increase of relative humidity corresponds to 50 g of water per hour per person and carbon dioxide to 0.1 m³ per hour per person. Half-times of the parameters during their decays were approximately twenty-four minutes, two hours, and five hours in the first six-hour period for air temperature, relative humidity, and carbon dioxide, respectively. The half-time for carbon dioxide is equivalent to the air exchange of the cave. However, to completely recover the ambient level of relative humidity and carbon dioxide, it took more than one and two days, respectively.

A larger decay rate of relative humidity following the exit of the visitors, in comparison to the decay rate of carbon dioxide indicates the absorption of some moisture by wall surfaces of the cave. However, due to the large hygroscopic capacity and surface area of the cave wall, as well as the high volume of air exchange with the dry outside air, the

Figure 12

Changes of air temperature, relative humidity, and carbon dioxide during controlled experiments conducted in Cave 323.



release of 500–700 g of moisture generated by visitors did not result in a noticeable increase of the baseline relative humidity in the cave. Furthermore, the natural influx of outside air dominated the cave's relative humidity before its complete recovery from the experiments.

Conclusions and Recommendations

The air temperature of Cave 335, which was closed to visitors, ranged from a low of 5 °C in February to the high of 19 °C in August, and the relative humidity varied between 19% in winter and 42% in summer. Outside air temperature and humidity ratios varied between –10 °C at 1.2 g of moisture per kg of dry air in February and 30 °C at 5.5 g of moisture per kg of dry air in August. The cave's natural moisture was removed throughout the year through constant flushing by the dry outside air. Therefore, moisture removal will be significantly reduced and the stability of the microclimate improved if the caves' entry doors are tightly sealed and access is tightly restricted to limit air exchange with the outside. If a

cave is completely sealed, it will maintain the natural relative humidity and temperature of the bedrock conglomerate, which is between 60% and 70% RH at 11–15 °C (Miura et al., herein).

The historical value and artistic quality of the artifacts at the Mogao grottoes have recently attracted many visitors each year. This trend will probably accelerate with the majority of tourists continuing to come in July through September and most of the visitors touring the grottoes in the morning. Visitors remain in a medium-size cave for an average of five minutes. At the present level of visitation, sixteen thousand visitors toured Cave 323 in the month of August. A significant accumulation of heat, moisture, and carbon dioxide—which can increase the rates of deterioration of the wall paintings and sculptures in the cave—was not observed, even during the high tourist season. However, visits to the cave did result in increased air-exchange rates, producing more unstable conditions in the cave. The visitors unknowingly brought a large amount of sand into the cave on their clothing and shoes, producing a dusty environment.

Although daily variations in environmental parameters caused by the visitors dissipated overnight, these visits generated sharp, twice-daily spikes of air temperature and relative humidity to +4 °C and $\pm 15\%$, respectively. These spikes were the result of large volumes of entrained outside air entering the cave as visitors entered. As expected, the spikes were larger near the entrance.

The presence of visitors often raised the carbon dioxide content of cave air to 2,000 ppm and occasionally to 3,000 ppm in August, although this figure always dropped to less than 750 ppm by the following morning because of the air-exchange rate. The American Society of Heating, Refrigeration and Air-Conditioning Engineers (ASHRAE) recommends a standard ventilation rate in public areas that will maintain the carbon dioxide level below 1,000 ppm (ASHRAE 1993). The continued entry of large numbers of visitors should be controlled, as undesirable health effects will result if the CO₂ level in a cave rises above 2,500 ppm.

Controlled experiments were conducted in Cave 323 to isolate the effects of a group of visitors on the microenvironments. The experiments yielded increased rates of temperature, relative humidity, and carbon dioxide during the group's stay as well as decay rates of these parameters following the visitors' exit from the cave. Generally accepted generation rates of moisture and carbon dioxide by adults (ASHRAE 1993) agreed with the measured values from the experiments. However, a large effect of entrained outside air during entry and exit was a major contributor of the perturbation of the microenvironment.

Twice-daily peaks of the environmental parameters can be controlled only by evenly distributing visits throughout the cave's open hours and limiting visitor access on days with extreme weather conditions, such as dust storms and heavy rain. Maintenance of the present air-exchange rate (approximately five hours during open hours) is important, as it is the only means of expelling moisture, carbon dioxide, and odor generated by visitors. The rate has been sustained even with the filter material—which had been installed to control wind-driven sand and airborne dust—

covering the louvers of the entry walls and doors. The unintentional transportation of sand into the cave by visitors can be easily controlled by requesting visitors to remove their shoes upon entry or placing a grate and floor mat outside of the cave.

Acknowledgments

The authors wish to thank Neville Agnew, associate director, programs, the Getty Conservation Institute, for his advice and discussion throughout the project. This work was conducted as an integrated part of the collaborative project between the State Bureau of Cultural Relics, the Dunhuang Academy, and the Getty Conservation Institute for the conservation of the Mogao grottoes.

References

- American Society of Heating, Refrigerating, and Air-Conditioning Engineers, Inc. (ASHRAE)
 1993 *ASHRAE handbook*. Atlanta: ASHRAE.
- Maekawa, S.
 1993 Environmental monitoring at the tomb of Nefertari. In *International Council of Museums (ICOM) Committee for Conservation 10th Triennial Meeting, Washington, D.C.*, 616-23. Paris: ICOM; Lawrence, Kans.: Allen Press.
- Torraca, G.
 1984 Environmental protection of mural paintings in caves. In *International Symposium on the Conservation and Restoration of Cultural Properties: Conservation and Restoration of Mural Paintings 1, Tokyo, 17-21 November, 1983*, 1-18. Tokyo: Organizing Committee of the International Symposium on the Conservation and Restoration of Cultural Property.